M-AM-Sym1 SOLVENT INDUCED INTERACTIONS AND STRUCTURE IN AQUEOUS SOLUTIONS. David Chandler, Department of Chemistry, University of Pennsylvania, Philadelphia, PA 19104, USA

This paper describes recent developments in the molecular theory of liquids as they pertain to solvation.

M-AM-Sym2 MOLECULAR DYNAMICS OF ION MOTIONS IN SOLUTION AND NEAR SOLUTION INTERFACES, M. A. Wilson, A. Pohorille, and L. R. Pratt

Common descriptions of ion motions near membranes or other supermolecular assemblies invoke conceptual simplifications involving brownian motion and continuum dielectric models. In the context of dynamics near surfaces, the regions of validity of these simple models have not been accurately determined. Fully molecular dynamical calculations are presented which are designed to test these simple models, and to provide molecular-level information on the dynamics of ions near aqueous solution interfaces.

M-AM-Sym3 LIGAND-RECEPTOR INTERACTIONS IN WATER. J. Andrew McCammon, Terry P. Lybrand, Michael H. Mazor and Chung F. Wong, Department of Chemistry, University of Houston, Houston, TX 77004.

Molecular dynamics computer simulations can provide detailed results on structural, thermodynamic and kinetic aspects of aqueous solutions. In particular, a new simulation approach called the thermodynamic cycle-perturbation technique allows one to calculate the relative free energy of binding for different ligand-receptor pairs in solution. Applications of these methods to ion-ionophore and inhibitor-enzyme pairs will be described, with special emphasis on structural and dynamic aspects of solvation and on the role played by solvation in molecular recognition and binding. This work has been supported in part by NSF (Biophysics Program and Office of Advanced Scientific Computing) and the Robert A. Welch Foundation. J.A. McC. is a Camille and Henry Dreyfus Teacher-Scholar. T.P.L. is the recipient of a Damon Runyon-Walter Winchell Cancer Fund Fellowship Award, DRG-888.

M-AM-Sym4 COMPUTER SIMULATIONS OF ORGANIC AND BIOMOLECULAR SYSTEMS IN SOLUTION. William L. Jorgensen, Department of Chemistry, Purdue University, West Lafayette, Indiana 47907.

Statistical mechanics simulations are being applied to study a wide range of problems concerning organic and protein chemistry in solution. By fitting to experimental data on liquids, intermolecular potential functions have been derived to describe the interactions between the components in the fluids. This includes a complete set of inter-peptide and peptide-water functions. The functions have been used in studies of the hydration of protein constituents, the hydrophobic effect and solvent effects on molecular conformation.

Furthermore, a combined quantum and statistical mechanics approach is being applied to study the effects of solvation on the energy profiles for organic reactions. The profile for the S_N2 reaction of $Cl^- + CH_3Cl$ in the gas phase has a double-well form with unsymmetrical ion-dipole complexes as minima and a symmetrical transition state. Hydration causes the reaction surface to become almost unimodal and increases the barrier significantly. However, in liquid DMF, the ion-dipole complexes are still free energy minima and the S_N2 reaction is not concerted. The addition reaction of $OH^- + H_2C{=}O$ has also been studied in the gas phase and in water. The substantial barrier in aqueous solution is essentially entirely solvent induced. For both reactions it is not so much a change in the number of solute-water hydrogen bonds along the reaction path, but rather in their strengths that is primarily responsible for the solvent induced barriers.

M-AM-A1 CHOLINERGIC RECEPTORS IN XENOPUS MYOCYTES: LARGER CONDUCTANCE CHANNELS HAVE LOWER AFFINITY FOR ACh. Anthony Auerbach and Christopher J. Lingle, Dept. Biophys. Sci., SUNY, Buffalo, NY. and Dept. Biol. Sci., FSU, Tallahassee, FA

At high ACh concentrations currents through single cholinergic receptors occur in bursts as channels enter and leave desensitized states. The figure shows the value of the predominant rate constant (λ) for open or closed intervals within bursts vs. [ACh]. For both 45 and 65 pS channels, the small decrease in the apparent closing rate (λ_o) with increasing [ACh] is due to missed short closures. For both forms of channel >.8 of detected closures were from the major component of the closed interval distribution (λ_c). 45 and 65 pS channels are similar in that λ_c increases as $[ACh]^{1.6}$ (2-100 μM ACh) and shows a tendency to saturate. The [ACh] at which $\lambda_c=\lambda_o$ (apparent K_d) is 8 μM for 45 pS and 20 μM for 65 pS channels. Differences in both open and closed intervals contribute to this difference in apparent K_d.

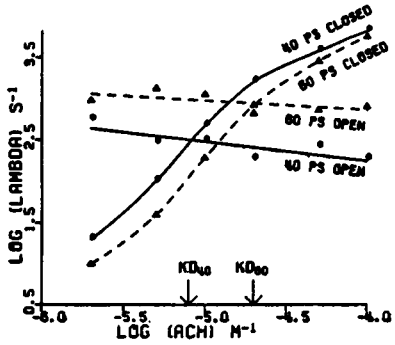

Assuming the standard model, these data indicate that binding (and perhaps gating) rates are different for the two conductance classes of channel. (Supported by MDA)

M-AM-A2 THE INHIBITION EFFECT OF ARSENICAL COMPOUNDS ON RAT BRAIN MUSCARINIC ACETYLCHOLINE RECEPTOR BINDINGS AND ACETYLCHOLINESTERASE ACTIVITY. El.A.M.Abdallah, F.A.Morsy, S.T.Eldeeb, and E.A.Kadous. Alexandria University, Faculty of Agriculture Dept. of Chemistry of Pesticide, ALEXANDRIA, EGYPT.

The inhibition effect of in vivo treatment with sodium arsenite, sodium methylarsonate(SMA), phenylarsonic acid(PAA), and benzylarsonic acid(BAA) on the binding properties of muscarinic acetylcholine receptors(AChR) in rat brain synaptosomes was investigated using the potent antagonist L-[^{3}H]quinuclidinyl benzilate ([^{3}H]QNB) to study binding to the muscarinic receptors, while 5,5-dithio-bis-(2-nitrobenzoic acid) (DTNB) was used for assaying acetylcholinesterase activity. At $5x10^{-3}$M,phenylarsonic acid caused complete inhibition of the [^{3}H]QNB binding. (SMA) and (BAA) caused less inhibition of [^{3}H]QNB binding than sodium arsenite; however the minimal inhibition effect of [^{3}H]QNB binding was observed when the arsenic element binded chemically with a methyl group in the case of sodium methylarsonate, while the chemical transformation of methylarsonate to benzylarsonic caused a maximal inhibition of [^{3}H]QNB binding of the rat brain muscarinic receptors. Also the results showed that inorganic arsenic and some organic ones especially when the element bind covalently with a methyl or a benzyl group in the form of SMA and BAA,they have a very weak inhibition effect on the [^{3}H]QNB binding. There was no relation between the effect of these arsenicals on (mAChR) and (AChE) activity,the I_{50} of sodium arsenite was($4.5x10^{-5}$M).

M-AM-A3 **HETEROGENEITY OF FUNCTIONAL NICOTINIC ACETYLCHOLINE RECEPTORS ON CLONAL CELL LINES IS REVEALED BY THE USE OF ^{86}RUBIDIUM ION EFFLUX STUDIES.** Ronald J. Lukas, Laboratory of Neurochemistry, Division of Neurobiology, Barrow Neurological Institute, 350 West Thomas Road, Phoenix, Arizona 85013.

The human medulloblastoma, TE671, and the rat pheochromocytoma, PC12, are continuous cell lines that have been used as models for central and autonomic nervous system neurons, respectively. Functional nAcChoR on TE671 and PC12 cells may be studied by the use of a $^{86}Rb^+$ ion efflux assay. In this assay, cells are loaded with $^{86}Rb^+$ via the action of the Na-K-ATPase, and extracellular isotope is removed. Functional nAcChoR-mediated responses are then assessed by quantitation of isotopic ion that is released from cells in a d-tubocurarine-sensitive fashion upon exposure to nicotinic cholinergic agonists.

Acetylcholine (in the presence of acetylcholinesterase inhibitors), carbamylcholine, and nicotine activate $^{86}Rb^+$ efflux from either TE671 or PC12 cells, while muscarinic receptor agents, amino acids and catecholamines are not effective. Alcuronium and pancuronium are nearly as potent as d-tubocurarine as antagonists of carbamylcholine-stimulated responses, while atropine is about 1000-fold less effective. Suberyldicholine and succinylcholine act as potent agonists on TE671 cells, but are antagonists at the nAcChoR of PC12 cells. A number of curaremimetic neurotoxins block functional nAcChoR-mediated responses of both cell lines, but show quantitative differences in antagonistic potency. This evidence for functional heterogeneity of nAcChoR complements other evidence for immunological and pharamcological heterogeneity of toxin binding sites on TE671 and PC12 cells.

M-AM-A4 TWO KINDS OF ACETYLCHOLINE-RECEPTOR CHANNELS AT SNAKE TONIC MUSCLE ENDPLATES.
V.E. Dionne, University of California, San Diego; La Jolla, California 92093

Acetylcholine receptor channels at garter snake tonic muscle fiber endplates were studied using patch-clamp methods. Whole muscles were removed from the animal, maintained in physiologic saline, and treated with collagenase plus protease to remove the nerve ending from the endplate membrane. Two types of agonist-activated channels were observed having different single channel conductances (nominally 42 and 30 pS; room temperature, cell-attached in normal saline). Both channel types had similar ion selectivities as judged by their reversal potentials (near 0 mV), both desensitized in the presence of acetylcholine, and both were found in the same membrane patches. Co-localization suggests that both types are endplate channels rather than channels of synaptic and non-synaptic origin. At low acetylcholine concentrations, the two channel types activated independently and randomly. At high concentrations, both channel types showed bursts of activity, but there was no interconversion and during a burst only one type was observed. The larger channel is similar to the single type of endplate channel found in twitch muscles in these animals. No physiological role for two kinds of endplate channels in slow fibers has yet been identified. [Supported by NIH:NS 15344]

M-AM-A5 A COMPARISON OF THE ACh CHANNEL BLOCKING ACTIVITY OF TWO ORGANOPHOSPHORUS ESTERS.
B. Cohen and C. Edwards, LCBG, NIADDK, NIH, Bethesda, MD. 20892

The effects of two organophosphorus esters (OPEs), dichlorovos (DDVP) and dicrotophos, on endplate currents and endplate current fluctuations in voltage clamped fibres of frog cutaneous pectorus muscles were compared. Three millimolar DDVP and dicrotophos similarly depressed endplate currents produced by 8 sec ionophoretic pulses of carbamylcholine but recovery from dicrotophos inhibition was much slower than from DDVP inhibition. Both OPEs depressed the amplitude of neurally evoked endplate currents (EPCs) reversibly at 1-3 mM but DDVP did so more effectively than dicrotophos unless the muscles were pretreated with methanesulfonyl fluoride (MSF) or DDVP, in which case their inhibitory effects were similar. MSF and DDVP are both irreversible anticholinesterases but have no irreversible effects on the ACh channel. The EPC decay was biphasic in 0.5-4 mM DDVP but not in 0.5-3 mM dicrotophos. The time constants of the EPC decay in 1-2 mM DDVP were not voltage dependent but the time constant in 3 mM dicrotophos showed the normal voltage dependence. Noise spectra were double Lorentzians in 0.5-1.0 mM DDVP and there was a significant reduction in the single channel conductance measured by noise analysis. Noise spectra in 0.5-2 mM dicrotophos were single Lorentzians with cut-off frequencies close to the control and there was no decrease in the single channel conductance in 0.5 and 1 mM dicrotophos. DDVP and dicrotophos blocked the ACh channel equally well during long agonist exposures but only DDVP affected the rate of channel closing and its voltage sensitivity. These OPEs seem to have similar affinities for the channel binding site(s) but DDVP reacts with the site(s) more rapidly than dicrotophos (supported by a contract from the U.S. Army Research Office, No. DAAG 2982K 0065).

M-AM-A6 TWO POPULATIONS OF ACETYLCHOLINE RECEPTOR CHANNELS AT THE NEUROMUSCULAR JUNCTION OF MATURE ADULT AND AGED RATS.
Dean O. Smith, Department of Physiology, University of Wisconsin, Madison, WI 53706. (Intr. by John W. Anderegg).

During the first three weeks after birth or following denervation, the gating properties of channels associated with the acetylcholine receptor at the rat neuromuscular junction change considerably. Specifically, the mean open time and the conductance of the channels decrease and increase, respectively. These properties have been further studied in mature (10 month) and aged (28 month) Fischer 344 rats and have been found to continue changing throughout the animals' lifetime. As a measure of mean channel open time, the decay time constant of extracellularly recorded miniature end-plate potentials was measured. A bimodal distribution of values was obtained; at 37°C, the modal values were 0.6 and 0.9 ms. The decay phase was well described by a double exponential curve in only 7% of the cases. Similar results were obtained from miniature end-plate currents and fluctuation analysis of acetylcholine-induced noise under voltage-clamped conditions; at room temperature, the modal values were about 1.3 and 2.0 ms, and less than 6% of the cases could be well fit by either a double exponential or double Lorentzian curve. In each of these experiments, about 62 to 63% of the channels in the 10-month rats had the relatively faster mean channel open times; in the 28 month animals, 31 to 47% had the faster values. Moreover, the channel conductances and single channel currents were unimodally distributed in the 10-month rats but bimodally distributed in the 28-month animals. Thus, two populations of channels are apparent in the adult rat, and the fraction of slower channels appears to increase with advanced age. Furthermore, there is apparently only one of the two channel types associated with an individual presynaptic release site. Supported by NIH grant AG01572.

M-AM-A7 **DISULFIDE CROSSLINK BETWEEN ADJACENT HALF-CYSTINYL RESIDUES AT THE ACETYLCHOLINE BINDING SITE.** **Peter N. Kao and Arthur Karlin. Departments of Biochemistry and Molecular Biophysics, and Neurology, Columbia University, New York, NY 10032.**

The nicotinic acetylcholine receptor contains a readily reducible disulfide bond at the periphery of the acetylcholine binding site. Reduction of this disulfide renders this receptor susceptible to affinity labeling with alkylating reagents containing quaternary ammonium moieties. We have used a radioactive form of one of these labels, 4-(N-maleimidobenzyltri-[^{3}H]-methylammonium ([^{3}H]MBTA), to locate the acetylcholine binding site on the α subunit of the receptor pentamer ($\alpha_2\beta\gamma\delta$) and to identify a particular pair of cysteinyl residues at this site. Four of the seven cysteines of Torpedo californica α (Cys 128, 142, 192, 193) occur in an N-terminal extracellular domain (Noda et al. Nature 299, 793, 1982). By protein microsequencing of a fragment of labeled α, we have shown that Cys 192 and Cys 193 are the residues specifically labeled by [^{3}H]MBTA (Kao et al. JBC 259, 11662, 1984). To identify all half-cystinyl residues at the acetylcholine binding site, we have now alkylated with a mixture of [^{3}H]MBTA and a nonspecific sulfhydryl reagent, N-[^{14}C]ethyl maleimide. Both labels were incorporated solely into Cys 192 and Cys 193; we observed no labeling of Cys 128 or Cys 142. In addition, from unreduced α, we have isolated two separate CNBr fragments, one containing Cys 128 and Cys 142 and the other containing Cys 192 and Cys 193. Each of these peptides contains an internal disulfide bond since only following reduction with dithiothreitol do they incorporate iodo[^{14}C]acetamide. Therefore Cys 128 is crosslinked to Cys 142, and Cys 192 is crosslinked to Cys 193. This latter unusual disulfide crosslink requires a cis peptide bond between Cys 192 and Cys 193.

M-AM-A8 DISTANCE BETWEEN THE LOCAL ANESTHETIC AND AGONIST BINDINGS SITES ON THE ACETYLCHOLINE RECEPTOR (AChR) DETERMINED BY FLUORESCENCE ENERGY TRANSFER. Jeffery M. Herz, David Johnson and Palmer Taylor, Div. Pharmacology, Dept. of Medicine, Univ. of California at San Diego, La Jolla CA. 92093 and Div. of Biomedical Sciences, Univ. of California, Riverside, CA. 92521

The AChR contains one agonist binding site on each of the two α-subunits and one allosterically coupled, high-affinity, local anesthetic binding site per receptor whose location is unknown. Fluorescence energy transfer has been used to map the distances between these sites. Fluorescent ligands for these sites were examined for site specificity, affinity, stoichiometry and capacity to effect a change in state. Ethidium was characterized as a probe of the local anethetic site by competition binding with [^{3}H]-PCP. In the presence of carbamylcholine, it binds with high affinity (K_D=0.36μM) while in the presence of α-toxin, ethidium binds with much lower affinity (K_D=1200μM). Binding of ethidium to the PCP site enhances [^{3}H] acetylcholine binding. Lifetime analysis and steady state titrations both show that ethidium exhibits a 14-fold increase in quantum yield upon binding to the local anesthetic site, and is completely displaced by other allosteric ligands: PCP, H_8-HTX and Dibucaine, at concentrations consistent with their independently determined K_D's. Fluorescence titrations in the presence of carbamylcholine yielded a K_D=0.25μM and a stoichiometry of one per receptor. Two fluorescence ligands, dansyl-C_6-choline (K_D=0.01μM) and NBD-bisquaternary acylcholine (K_D=0.22μM) were used as probes of the agonist binding sites. Fluorescence energy transfer determined by steady state and lifetime analysis indicated that the minimum distance between these sites is ∿55A. The results allow a prediction of the position of the local anesthetic site relative to the plane of the membrane. Grant GM24437 and DAMD-178C4187.

M-AM-A9 **FREE ENERGY PROFILE: ION CHANNEL ACETYLCHOLINE RECEPTOR**

Paul A. Bash, Robert Stroud, Robert Langridge, U. C. Singh, Peter Kollman
University of California, San Francisco

A molecular model of the ion channel in the acetylcholine receptor (ACHR) has been built and the free energy barrier to ion flow is calculated from this model. This energy profile is first estimated by determining the partition function on 0.5*x* 8.0*x* 8.0 angstrom slices along the length of a fixed channel model. When this calculation is carried out at a dielectric constant of 80, the energy barriers are in reasonable agreement with experiments which indicate a free energy barrier of about 3-5 *kcal/mol*. Although the channel has been shown to be water filled, the effective dielectric constant is not known. Therefore, a more detailed calculation that makes no assumption about the dielectric properties in the channel must performed. The potential of mean force that an ion would feel due to the environment in the channel is calculated by determining the frequency distribution of an ion along the channel. Molecular dynamics with umbrella sampling is utilized to generate the necessary statistics. One ion, 100 water molecules, and the 30 amino acid residues in the immediate vicinity to the ion are permitted to move during the simulation. The resultant energy profile is compared with the calculation using a fixed channel and flux measurements from electrophysiology. The methods described above provide the means to investigate the properties of an ion channel in a transmembrane protein at the molecular level.

M-AM-A10 VOLTAGE-GATED, HIGH CONDUCTANCE SINGLE CHANNELS FROM ADULT XENOPUS LAEVIS MYOTUBES IN CULTURE. Craig A. Bogen and Solomon D. Erulkar (Intr. by C. Franzini-Armstrong). Departments of Neurology and Pharmacology, Univ. of Pennsylvania, Philadelphia, PA 19104.

Large conductance voltage-dependent single channel currents have been recorded using patch clamp techniques from surface membrane of myotubes cultured from laryngeal and quadriceps muscle of adult Xenopus laevis. In inside-out membrane patches, conductances ranging from 330-410 pS have been measured in symmetric solutions containing (mM): 116NaCl; 2KCl; 1.8$CaCl_2$; 5HEPES; 5.6 glucose; pH 7.3. Channels were open within a narrow window of steady-state potential ranging from approximately -25 to +10mV; outside of this range, they were inactivated. The majority of the channels were highly permeable to chloride, to a lesser degree isethionate, and impermeable to gluconate. These channel properties are similar to those reported for channels from cultured rat myotubes (Blatz, A.L., and K.L. Magleby, 1983. Biophysical J., 43: 237-241) and cultured rat Schwann cells (Gray, P.T.A., S. Bevan, and J.M. Ritchie, 1984. Proc. R. Soc. Lond., 221: 395-409). Significant potassium and smaller sodium conductances were also measured. A small number of channels opened in response to the presence of low concentrations of free calcium at the cytoplasmic face of the membrane and closed when the concentration was reduced to values lower than 25nM. In myotubes grown in culture for less than 25 days, the high conductance channels were present in 73% (33/45) of the patches obtained; in myotubes grown for 26-41 days, the channels were present in only 50% (22/44) of the patches. It is uncertain whether this change represents a difference in channel density or a change in activation properties of channels in cells of different age. (Supported by NIH grants NS12211 and NS07510-01).

M-AM-A11 VOLTAGE CLAMP AT GLUTAMATE RESPONSIVE SYNAPSES IN DROSOPHILA. James McLarnon and David M. J. Quastel, Department of Pharmacology & Therapeutics, Faculty of Medicine, The University of British Columbia, Vancouver. B. C., CANADA, V6T 1W5.

At present relatively little is known regarding the kinetics of drug interactions with the receptor-ion channel complex at glutamate responsive synapses. Unlike the mammalian neuromuscular junction, the glutamate-sensitive neuromuscular junctions in insects and crustaceans have not proven particularly amenable to analysis using point voltage-clamp. Recently we have been able to apply both the single-electrode and two-electrode point voltage-clamp to ventral longitudinal muscle fibers in drosophila larvae, where previous work has shown these fibers to be responsive to glutamate. In preliminary studies we have found that the decay time course (which is close to exponential) of the miniature excitatory junctional currents (MEJCs), to be considerably prolonged compared to those reported for MEJCs in locust and crab muscle; at room temperature and a holding potential of -80 mV, the decay time constant is near 18 ms. Individual MEJCs in drosophila show a considerable variation in time course similar to that exhibited at the mouse neuromuscular junction after poisoning of acetylcholinesterase. The height of the MEJC is about 2 nA at -80 mV and increases with membrane hyperpolarization; the extrapolated reversal potential is about -10 mV. The application of ethanol (0.4 M) or dimethylsulfoxide (4% by volume), agents which prolong the miniature endplate current at the mouse neuromuscular junction, had little effect on the time course of MEJCs but caused a doubling in the frequency of the MEJCs, a presynaptic action which is somewhat less than that observed at the mouse nerve terminal.

M-AM-A12 CAT-50: A CATION-SELECTIVE CHANNEL FROM FROG LENS EPITHELIUM. K.E. Cooper, J.M. Tang, J.L. Rae and R.S. Eisenberg, Department of Physiology, Rush Medical College, Chicago, IL

Patch clamp recording from the apical surface of the epithelium of frog lens reveals a cation selective channel ("CAT-50") after pressure (about ± 30 mm Hg) is applied to the pipette. The open state of this channel has a conductance of some 50 pS near the resting potential (-50 mV in these isolated epithelia) when the pipette is filled with 107 mM NaCl and 10 mM HEPES, PH 7.3. The probability of the channel being open is strongly dependent on pressure but the current-voltage relation of the open state is not affected by pressure: it is nonlinear even in symmetrical salt solutions, allowing more current to flow into the cell than out. Interestingly, similar channels seen in excised patches can be quite linear. The CAT-50 channel is selective when substantial inward currents flow, with $K \gtrsim Rb \gtrsim Cs > Na > Li$, but it distinguishes much less when little current flows. The conductance depends monotonically on the mole fraction of K when the other ion present is Li or Na, suggesting that the pore may be occupied by only one ion at a time. Eyring rate theory has been used to predict conduction through a single-ion channel with fixed energy barriers. The theory predicts that the current through an open channel is a saturating monotonic function of permeant ion concentration. CAT-50 shows this behavior at least up to 214 mM K. CAT-50 shows little sign of rapid closings to baseline when open in solutions containing only monovalent ions, but these are prominent when the pipette contains divalent ions (Ba or Ca) or elevated H_3O^+. The surprisingly high noise level of the current through the open channel, particularly at low frequencies, invites investigation.

M-AM-B1 ST-EPR AS A PROBE OF THE DYNAMIC CONFORMATIONAL STATE OF CROSSLINKED ACTO-S1 IN THE PRESENCE OF NUCLEOTIDES. Eric C. Svensson and David D. Thomas, Dept. of Biochemistry, University of Minnesota Medical School, Minneapolis, MN 55455.

We have used saturation transfer electron paramagnetic resonance (ST-EPR) to study the rotational dynamics of crosslinked acto-S1 (XLAS1), in which S1 was spin-labeled at the SH1 thiol and crosslinked to actin using 1-ethyl,3-(3-dimethylaminopropyl)carbodiimide. Our previous work on this system (1985, Biophys. J. 47:467a) showed that the rotational mobility of XLAS1 is identical to that of uncrosslinked acto-S1 in the absence of nucleotide, suggesting that crosslinking does not affect the conformation of acto-S1. In the presence of ATP, the rotational mobility increased dramatically. In the present study, in order to ask whether this motion requires an active ATPase cycle, we have investigated the effects of nucleotide analogs. ATP-γS and AMP-PNP + 50% glycol increase the rotational mobility of XLAS1, with effects similar to that of ATP, and they both cause complete dissociation of acto-S1 (200 μM actin, 100 μM S1, 5 mM nucleotide, μ = 180 mM, 1 mM Mg^{++}, 20°C). Thus a cycling ATPase enzyme is not necessary to induce microsecond rotational motions in XLAS1. However, ADP + 0.5 M KCl has no effect on the rotational mobility of XLAS1, even though it causes greater than 50% dissociation in uncrosslinked acto-S1, as measured by ST-EPR. Thus a substantially weakened acto-S1 interaction is not sufficient to induce microsecond mobility in XLAS1. Two likely interpretations will be discussed: (1) we have detected the rotational mobility that would occur in a weakly attached state in an active muscle fiber, and (2) the mobile heads in an active fiber are all detached.

M-AM-B2 THE ACTIVE FORCE GENERATING ELEMENTS OF MUSCLE CROSS-BRIDGES ARE CONFINED TO THE HEAD OF THE MYOSIN MOLECULE. A. J. Baker and R. Cooke. Department of Biochemistry & Biophysics, and the CVRI, University of California, San Francisco, CA 94143-0448.

The location and nature of the contractile events within the actomyosin complex are as yet undefined. Within a myosin crossbridge two putative sites for energy transduction have been considered. The first proposes that S1 or some domain of S1 experiences a change in orientation during the powerstroke. The second proposes that a region of S2 which connects S1 to the thick filament is shortened by a helix to random coil transition. Several studies have shown that exposure of fibers or myofibrils to the bi-functional reagent dimethyl suberimidate (DMS)(5mm, pH 7.0, 0°C) for 5 hours causes approximately 80% of S2 fragments to be cross-linked back onto the thick filaments from which they project (K. Sutoh and W.F. Harrington (1977) Biochem. 16, 2441). The mechanical and enzymatic properties of glycerinated muscle fibers were measured following DMS treatment. The degree of cross-linking of S2 to the thick filament was as previously reported. Our results have shown that ATP hydrolysis, force generation and shortening can still occur in fibers after the S2 region of myosin has been chemically cross-linked to the thick filament. These data place several restrictions on models of contraction and specifically exclude those that involve: large scale shortening of S2; azimuthal motions of attached cross-bridges around the actin thin filament; or those that require extensive movements of the crossbridge out from the thick filament during its cycle. Supported by grants from the USPHS AM30868 and HL32145. A.J.B. is a California Heart Association Fellow.

M-AM-B3 THE NUCLEOTIDE SITE OF MYOSIN DOESN'T ROTATE DURING THE POWERSTROKE. M. Crowder and R. Cooke. Department of Biochemistry & Biophysics, and the CVRI, University of California, San Francisco, CA 94143-0448 and IBM Instruments Inc., San Jose, CA 95110.

Spin-labeled analogs of ATP have been used to measure the orientation of the nucleotide site of myosin in glycerinated rabbit soleus muscle. Three analogs have been synthesized with the spin label attached to the 3' position of 2'dATP (3'SL-ATP), to the 2' position of 3'dATP (2'SL-ATP) or to either position of ATP (SL-ATP). Diphosphate analogs bound to muscle fibers are highly ordered with gaussian spreads of angles, 15° FWHM, centered at 45° (2'SL-ATP) or 63° (3'SL-ATP) relative to the fiber axis. The rate of hydrolysis of the analogs by myofibrils was 75% of that measured for ATP. All three analogs (50 - 250 μM) supported high tensions (120% of that for ATP) but velocities of contraction were inhibited by 50%. EPR spectra obtained from active fibers in 50 - 250 μM analog displayed peaks characteristic of the orientation of diphosphate analogs as well as an isotropic component characteristic of myosin heads that are not bound to actin. No new well-defined orientations were seen. These results suggest that the nucleotide site on myosin doesn't rotate during the powerstroke, a conclusion similar to that drawn from the spectra of spin probes attached to a reactive sulfhydral and from fluorescent nucleotides also bound to the nucleotide site on myosin (Yanagida, J. Mus. Res. Cell Mot. 6:43, 1985). Supported by a grant from the USPHS: AM30868.

M-AM-B4 FRACTION OF MYOSIN CROSS-BRIDGES BOUND TO ACTIN IN ACTIVE MUSCLE FIBERS: ESTIMATION BY FLUORESCENCE ANISOTROPY MEASUREMENTS. Thomas P. Burghardt and Katalin Ajtai. CVRI, U.C., San Francisco, San Francisco, California 94143.

Time-resolved and steady-state fluorescence anisotropy measurements from fluorescence-labelled myosin cross-bridges in single glycerinated skeletal muscle fibers in rigor, relaxation, MgADP-induced, and contraction have been made to estimate the fraction of actin bound cross-bridges in active muscle. When the plane of polarization of the excitation light is perpendicular to the fiber axis and its propagation vector has a component parallel to this axis, actin-bound cross-bridge states, such as rigor and MgADP-induced, have time-zero and steady-state anisotropies that are substantially lower than the relaxed state. This difference provides a means of determining the fraction of cross-bridges bound to actin in active isometric fibers by comparing the fluorescence anisotropy from active fibers with the anisotropy from bound and unbound cross-bridges in static states. By assuming that the active cross-bridges are either bound (in the manner of rigor or MgADP-induced) or relaxed, we estimate that more than 80% of the cross-bridges are actin-bound in active isometric fibers. This research was supported by grants from the U.S.P.H.S. HL-16683 and from the Muscular Dystrophy Association.

M-AM-B5 OBSERVATION OF TWO ORIENTATIONS FROM RIGOR CROSS-BRIDGES IN GLYCERINATED MUSCLE FIBERS. Katalin Ajtai and Thomas P. Burghardt. CVRI, U.C., San Francisco, San Francisco, California 94143.

The fluorescence polarization from rhodamine labels specifically attached to the fast reacting thiol of the myosin cross-bridge in glycerinated muscle fibers has been measured to determine the angular distribution of the cross-bridges in different physiological states of the fibers as a function of temperature. To investigate the fibers at temperatures below $0^{o}C$ we have added either glycerol or ethylene-glycol to the bathing solution as an antifreezing agent. We find that the fluorescence polarization from the rhodamine probes detects distinct angular distributions of the cross-bridges in isometric-activity, rigor, MgADP, and low ionic strength relaxed fibers at $4^{o}C$. We also find that the rigor cross-bridges in the presence of glycerol or ethylene-glycol can maintain at least two distinct orientations relative to the actin filament, one dominant at temperatures $T>2^{o}C$ and another at $T<-10^{o}C$. MgADP cross-bridges in the presence of glycerol maintain approximately the same orientation for all temperatures investigated. The rigor cross-bridge orientation at $T<-10^{o}C$ is similar to both the MgADP cross-bridge orientation in the presence of glycerol and the active muscle cross-bridge orientation at $4^{o}C$. These findings show that the rigor cross-bridge in the presence of glycerol or ethylene-glycol has at least two distinct orientations while attached to actin: one of them dominant at high temperature, the other dominant at low temperature or when MgADP is present. The latter orientation resembles that present in isometric active fibers. These findings suggest that force generation in the activated cross-bridge cycle may occur as a result of an actin attached cross-bridge transition between these two orientations. Research supported by USPHS grant HL-16683 and by the Muscular Dystrophy Association.

M-AM-B6 KINETICS OF CYCLING CROSS-BRIDGES IN ACTIVE MUSCLE DERIVED FROM MEASUREMENTS OF ISOMETRIC FORCE, RATE OF FORCE DEVELOPMENT, AND ISOMETRIC ATPase.
Bernhard Brenner, Institute of Physiology II, University of Tübingen, FRG.

Recently we described a new experimental protocol which allows to measure the rate of force development in skinned muscle fibers while the contractile material is constantly activated (Brenner, B., Biophys. J., 1984). Parallel measurements of the rate of force development, isometric force, and isometric ATPase allow to determine the apparent rate constants for (a) the transition of cross-bridges from the non-force generating state(s) to the force generating state(s), and (b) the transition from the force generating state(s) back to the non-force generating state(s). Since these two apparent rate constants are the equivalent of the attachment rate constant 'f' and detachment rate constant 'g' of the original two-state model of A.F. Huxley (Prog. Biophys. biophys. Chem., 1957) they will be called '$f_{app.}$' and '$g_{app.}$' respectively. The two apparent rate constants were determined at various MgATP concentrations. It is found that MgATP apparently only affects '$g_{app.}$'. Furthermore, at $5^{o}C$, ionic strength 0.17, and 5mM MgATP '$f_{app.}$' is found two to three times as large as '$g_{app.}$'. This means that at any time 2/3 to 3/4 of the cycling cross-bridges are attached in the force generating states. Since this agrees well with stiffness measurements in active fibers compared to rigor where presumably all cross-bridges are attached these findings suggest that all cross-bridges are recruited in active muscle with 2/3 to 3/4 attached in the force generating states. Since raising temperature results in a more than 2-fold increase in isometric force an increase in average force/cross-bridge with temperature has to be postulated. Further experiments are needed to decide whether this might reflect temperature dependence of an equilibrium between force generating states producing various amounts of tension. (DFG Br 849/1-1)

M-AM-B7 KINETICS OF CYCLING CROSS-BRIDGES IN ACTIVE MUSCLE. THE EFFECT OF CALCIUM CONCENTRATION. Bernhard Brenner, University of Tübingen, FRG. (Sponsored by J.H. Miller)

Kinetics of cycling cross-bridges in active muscle were derived from parallel measurements of the rate of force development (Brenner, B., Biophys. J., 1984), isometric force, and isometric ATPase. The two key rate constants for cycling cross-bridges, '$f_{app.}$' and '$g_{app.}$' (see Brenner, B., this meeting), were determined at various sarcoplasmic Ca^{++} concentrations. It is found that Ca^{++} strongly affects '$f_{app.}$', the apparent rate constant for the transition from the non-force generating states to the force generating states, while '$g_{app.}$', the apparent rate constant for the transition from the force generating states back to the non-force generating states is almost unaffected. This implies that the fraction of cycling cross-bridges found in the force generating states increases with Ca^{++} concentration. It follows that the increase in isometric tension with sarcoplasmic Ca^{++} concentration is not only the result of the well known increase in the number of activated interaction sites (cycling cross-bridges), but also the result of an increasing fraction of cycling cross-bridges in the force generating states. Comparison of isometric force with the fraction of cycling cross-bridges in the force generating states allows to calculate the number of activated interaction sites (cycling cross-bridges) at the various Ca^{++} concentrations. Due to the effect of Ca^{++} on '$f_{app.}$' it is found that compared to the number of activated interaction sites isometric force starts to increase at significantly higher Ca^{++} concentrations. When Ca^{++} binding to the regulatory proteins is compared with the resulting isometric force the described effects of Ca^{++} on kinetics of cycling cross-bridges have to be considered. These experiments demonstrate that besides other possible mechanisms regulation of muscle involves control of the rate constant of the transition from the non-force generating states to the force generating states by Ca^{++}. (DFG Br 849/1-1)

M-AM-B8 ATP HYDROLYSIS RATE AND CROSSBRIDGE KINETICS AS FUNCTIONS OF IONIC STRENGTH AND PHOSPHATE ION CONCENTRATION IN CHEMICALLY SKINNED RABBIT PSOAS FIBERS. M. Kawai* and K. Güth#. *Department of Anatomy and Cell Biology, Columbia University, New York, N.Y. 10032, U.S.A.; #II Physiologisches Institut, Universität Heidelberg, 6900 Heidelberg 1, F.R.G.

The ATP hydrolysis rate was measured by the PEP-NADH fluorescence method, and the results were correlated with crossbridge kinetics obtained from the tension transients in response to sinusoidal length alterations. When the ionic strength (I.S.) was increased from 100mM to 300mM, there was a progressive decrease in the isometric tension (60%) and in ATPase rate (30%). Crossbridge kinetics were not altered as indicated by the 3 rate constants (a, b, c) which remained the same as I.S. was changed; oscillatory power output decreased because of the proportionate decrease in the magnitude of the rate constants. When phosphate (Pi) concentration was increased in the range 0mM to 16mM at constant I.S.(200mM), tension decreased by 50% and ATPase by 20%. In contrast to the I.S. effect, changes in Pi concentration caused a significant increase in the rate constant b (2.5X) and its magnitude (2X), resulting in 5-fold increase in the oscillatory power output. The effect was greater at higher amplitudes (up to 0.5% peak-to-peak), without visible increase in ATPase rate. The I.S. effect can be explained in terms of shifting the rapid equilibrium between attached and detached states of crossbridges, where higher I.S. favors more detached states. The Pi effect is more complex and cannot be explained by merely reversing the Pi release step; our results imply an additional site of action for Pi that can improve the efficiency of oscillatory power production.

M-AM-B9 TIME-RESOLVED STUDIES OF THE RELATION BETWEEN FORCE REDEVELOPMENT AND STIFFNESS IN SINGLE INTACT FIBERS OF THE FROG. J. Gulati and A. Babu (Intr. by T. Robinson), Departments of Physiology and Medicine, Albert Einstein College of Medicine, Bronx, NY 10461.

The study was made to determine the rate constant for cross-bridge attachment in vivo, since this parameter is important in the cross-bridge theories of muscle contraction. Single fibers were isolated from the frog tibialis muscle and stimulated tetanically (40 Hz pulses) at 0°C and 2.2 um sarcomere length. During the force plateau, the fiber was released by 20%Lo to a slack length. A part (approx. 10%Lo) of the slack was allowed to be absorbed by the intrinsic contraction with unloaded shortening speed, following which the fiber was stretched back to the original length (2.2 um). The time course of force redevelopment at this fixed length was followed and the stimulation was then ended. In the next contraction, the same sequence was repeated except that, in addition, the fiber length was continuously oscillated (sinusoidal waveform, 0.5-2.5 kHz, 0.1-0.3%Lo peak to peak), which gave the measurement for the change in fiber stiffness accompanying the force. The rate constant for the stiffness change was taken as the best estimate for cross-bridge attachment ($33\ sec^{-1}$). This moderate value for the attachment rate is consistent with the view that force transduction by the cross-bridge is completed in a series of elementary chemo-mechanical steps, in the turnover cycle, starting with the attachment. The time resolution of the data for force and stiffness recoveries after stretching also indicated a significant lead for the cross-bridge attachment over the development of tension, which provides evidence for the existence of a zero- (and/or, low-) force attached state in the cross-bridge cycle in the presence of maximal, nearly steady, level of calcium, in vivo. [Supported by National Science Foundation (PCM-8303045)]

M-AM-B10 RELAXATION AND INITIATION OF ACTIVE CONTRACTION OF RABBIT SOLEUS MUSCLE FIBERS BY CAGED ATP PHOTOLYSIS M.Yamakawa*, K.W.Ranatunga+, and Y.E.Goldman* Dept. of Physiol.*, Univ. of Penna., Phila., PA. 19104 and Dept. of Physiol.+, Univ. of Bristol, Bristol BS8 1TD, England.

We compared the kinetics of relaxation and activation of contraction following laser pulse photolysis of caged ATP in rabbit slow-twitch soleus muscle with previous measurements on rabbit fast-twitch psoas muscle. Single glycerol-extracted fibers were put into a rigor solution containing (mM): 100 TES, 1 free Mg^{2+}, 53 EGTA, 10 glutathione, 200 total ionic strength, pH 7.1 at 21 °C. Caged ATP, 10 mM was then added. Following liberation of ~0.7 mM ATP by a 347 nm laser pulse (figure, arrow) in the absence of added Ca^{2+}, tension decreased to the relaxed level. When the fiber was stretched by 0.6% (s) 0.5 s before laser pulse, the tension trace converged with that of an isometric trial (i) well before final relaxation, indicating transient cross-bridge reattachment and force generation (Goldman et al., J. Physiol. 354:577, 1984). The presence of 10 mM P_i increased the rate of final relaxation as occurs in psoas fibers (Hibberd et al., Science 228:1317, 1985). 10 mM P_i also decreased the half-time for convergence of (i) and (s) which does not occur in psoas. In the presence of ~30 μM free Ca^{2+}, liberation of ~0.7 mM ATP caused a decrease in tension followed by development of active contraction. Fitting a simple kinetic model (Goldman et al., J. Physiol. 354:605, 1984) to the soleus tension transients, gave values of ~2 x 10^4 $M^{-1}s^{-1}$ for the apparent second order rate constant of ATP-induced dissociation of rigor cross-bridges and ~75 s^{-1} for the subsequent reattachment to produce active force. Compared to psoas fibers the rate constant for ATP-induced detachment in soleus is decreased more than that for reattachment. M.Y. is an MDA postdoctoral fellow. Supported by MDA, NIH grant HL15835 to the Penna. Musc. Inst., and AM26846.

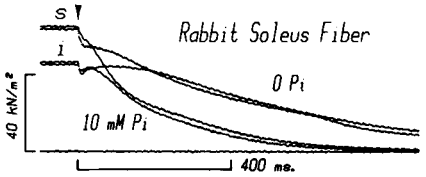

M-AM-B11 INORGANIC PHOSPHATE EFFECTS ON CONTRACTION OF FAST AND SLOW MUSCLE FIBERS. P.B. Chase and M.J. Kushmerick, Dept. of Radiology, Brigham & Women's Hospital, Boston, Mass. 02115.

Muscle intracellular [Pi] can vary *in vivo* by over an order of magnitude. During tetanic contraction, [Pi] increases; isometric force (F_{iso}) and unloaded shortening velocity (V_{us}) decline in fast vertebrate skeletal muscle, but F_{iso} and V_{us} do not change in slow muscle. As one product of the myosin ATPase reaction, Pi may significantly affect contraction. However, other changes occur *in vivo* in parallel with increasing [Pi]. Therefore, to study Pi effects on contraction in an otherwise constant medium, we used single glycerinated fiber segments from rabbit psoas (fast) and soleus (slow) muscles. [Pi] was varied from 0.1-30 mM.

We observed qualitatively similar results in both fiber types (full activation; 12°C): (1) F_{iso} declined as [Pi] increased by almost 50% over the range studied; (2) Bode analysis of stiffness, using small (< 0.05% L_o) sinusoidal length changes (freq = 0.5-200 Hz), showed that increased [Pi] shifted oscillatory work to higher frequencies and increased the stiffness relative to force; and (3) V_{us} depended little, if at all, on [Pi].

[Pi] increase is a factor in decreasing F_{iso} of intact fast muscle. The results predict a smaller decrease in F_{iso} of slow muscle *in vivo*, due to higher basal [Pi] and a smaller relative [Pi] change, but do not explain the constant F_{iso}. Increased [Pi] cannot explain the decreased V_{us} of fast muscle *in vivo*. Because V_{us} does not depend on [Pi], [Pi] does not affect the rate limiting step of myosin ATPase in the steady state. Bode analysis demonstrates that [Pi] alters some kinetic parameter(s) involved in force generation.

Supported by NIH grant AM-32018.

M-AM-B12 NO TENSION FLUCTUATIONS DURING LARGE SLOW STRETCH AND RELEASE IN RAT PSOAS MYOFIBRILS. Tatsuo Iwazumi, Dept. of Medical Physiology, Univ. of Calgary, Calgary, Alberta T2N 4N1

It was reported previously (Iwazumi, Biophys. J. 45: 158a) that, during isometric contractions elicited by Ca^{++}, bullfrog atrium myofibrils did not produce spontaneous tension fluctuations at the system detection limit of 0.5 ng/√Hz. Since it is conceivable that the cross-bridge cycling might be arrested during highly isometric contraction or that the bullfrog myofibrils might have peculiar properties, we have made spontaneous noise measurements on rat psoas myofibrils during contraction undergoing slow stretches and releases of 1 sec interval each. To maximize the amplitude of stretch and release per sarcomere (greater than 5 %), myofibril lengths were made as short as possible (the shortest one had only 9 sarcomeres). Fewer number of sarcomeres is also advantageous in increasing the fluctuation magnitude.

The tension responses to slow stretches and releases were slightly curved triangular waves with very smooth appearance; no kinks were observed after a brief transient at every directional change. The noise spectra taken during later 0.5 sec of the stretch and release were identical to those obtained during rest; no spontaneous fluctuations were present above system noise floor. It is, therefore, concluded that the lack of spontaneous fluctuations during isometric contractions observed previously was not due to cross-bridge lock-up nor ATPase cessation nor peculiarity to the bullfrog atrial myofibrils. Supported by Muscular Dystrophy Association.

M-AM-B13 ANALYSIS OF TENSION NOISE IN KINETIC MODELS OF MUSCLE CONTRACTION. by J.P. Payne, G.H. Templeton, and T. Iwazumi*. Dept. Physiology, Univ. Tex. Health. Sci. Center at Dallas, Dallas, TX 75235 and *Dept. Medical Physiology, Univ. Calgary, Calgary, AL, Canada.

Spontaneous tension fluctuations are expected from stochastic cross-bridge cycling during active contraction. We have reported that no tension fluctuations can be detected during isometric and slow auxotonic contractions of healthy isolated skeletal and cardiac myofibrils. For tension fluctuations to remain thus unobserved, the cross-bridge attachment rate must be at least three orders of magnitude greater than the detachment rate; indicating that isometric turnover might be exceedingly slow. To examine this possibility, we derived the expected noise power spectra for a number of linear, kinetic cross-bridge models. Such models describe the cross-bridge as cycling through a series of discrete biochemical/mechanical states with the transitions governed by first-order rate constants. In addition, the effect of conduction of such tension fluctuations along a myofibril to the force transducer was calculated. Results from these calculations from various models showed that for a fully activated half-sarcomere, the rms tension fluctuation was between 0.3-1.0% of isometric tension, and the calculated fluctuation relaxation time between 1-20 ms. The total rms fluctuation for a myofibril was the value for a half-sarcomere times the square root of serial sarcomeres. Using Huxley's model (Prog. Biophys.,7,255), from our measured value Po = 50 ug, and Vmax = 5 l/sec (Tarr et al., Circ. Res., 48,189), and assuming w/e = 0.75, we determined that: f1 = 1.5/s, g1 = 0.0015/s, g2 = 150/s, a/Po = 0.0013, Jo = 0.0002/s, and Jmax = 0.2/s. Clearly, these values do not meet with reported values for striated muscle kinetics; therefore, another explaination for the lack of tensio fluctuations must be sought. Supported by MDA, NASA, and N.I.H.

M-AM-C1 COMPONENTS OF ASYMMETRIC CHARGE MOVEMENT IN CONTRACTING SKELETAL MUSCLE FIBRES OF THE RABBIT. G.D. Lamb (Intr. A. Martin), Dept. of Physiology, JCSMR, ANU, Canberra, ACT, 2601, Australia.

The vaseline-gap clamp was used to record asymmetric charge movement in white sternomastoid (s.m.) or soleus fibres of the rabbit. The holding potential was usually -90mV. At 22°C, non-linear ionic currents were virtually eliminated by the solutions used. Internal solution (mM): 148 Na glutamate, 1 Mg glutamate, 10 TES, 0.5 Na_2 ATP, pH 7.0. Cs^+ replaced Na^+ in some experiments. External solution (mM): 150 TEABr, 0.2 $CaSO_4$, 8$MgSO_4$, 2.5 2,4 dichlorophenoxyacetic acid, 2 TES, 10^{-3} TTX, pH 7.2. Addition of 80 mM sucrose to the external solution increased the speed of both a) the asymmetric charge movement and b) the charging of the linear capacitance of the fibre. The linear relationship between these two variables strongly indicated that at least the majority of the charge movement resided in the transverse tubular system. A hump, analagous to q_γ in amphibia, was seen on the ON charge near the contraction threshold in some fibres. Nifedipine (2 to 10μM) decreased the maximum asymmetric charge by between 25 and 80% in every s.m. (21) and every soleus (4) fibre examined. Nifedipine did not affect the charge moved by small depolarizing steps (to below -50mV), and the charge remaining after addition of nifedipine saturated near -20mV. D600 (methoxyverapamil, 30μM) had a similar effect. As both drugs block calcium currents in these concentrations, it is proposed that the surpressed charge movement is a calcium gating current. Contraction was usually not affected by these drugs.

M-AM-C2 VOLTAGE DEPENDENT CAPACITANCE OF FROG SKELETAL MUSCLE FIBERS MEASURED USING FREQUENCY-DOMAIN TECHNIQUES. J.A. Heiny and F. Bezanilla, Dept. of Physiology & Biophysics, U. of Cincinnati, Cincinnati, OH, and Dept. of Physiology, U.C.L.A., Los Angeles, CA.

The membrane admittance of frog skeletal muscle fibers was measured under voltage-clamp conditions and in the absence of ionic conductances, for membrane potentials between -120 and 0 mV. Standard time-domain records of non-linear charge movement currents were recorded from the same fibers using P/4 subtracting pulse protocols. Fibers were voltage-clamped using a vaseline gap method (Hille & Campbell, 1976) and the admittance was measured under steady-state conditions using a small signal (2-4 mV) pseudorandom white noise stimulus superimposed on the holding potential (Fernandez et al., 1982; Stimers et al., 1985). The membrane capacity was found to be both voltage and frequency dependent. The voltage-dependent part of the membrane capacitance, obtained by subtracting the capacitance measured at hyperpolarizing holding potentials from that at depolarizing potentials, had a maximum near D.C. and declined monotonically with increasing frequency. The peak capacitance followed a bell-shaped curve, with a maximum change of 2-4 uF/cm2 at about -70 mV.

Supported by the E. Lapp Foundation, U. of Cincinnati College of Medicine, and grants from M.D.A. and N.S.F. (RII-8508305).

M-AM-C3 MEMBRANE CURRENTS AND INTRAMEMBRANE CHARGE MOVEMENT IN NON-POLARIZED SKELETAL MUSCLE FIBERS. INACTIVATION WITHOUT CHARGE IMMOBILIZATION. G. Brum and E. Rios. Department of Physiology. Rush Medical School, Chicago.

Membrane currents were recorded from single cut fibers of frog skeletal muscle under voltage clamp. Non-polarized fibers in solutions with K and Na channel blockers showed inward currents upon application of pulses to large negative voltages. These currents decayed during the pulse with a markedly voltage-dependent rate, were reduced by low Ca external solutions and essentially eliminated by a solution with EGTA, sulfate and Cd. They may be deactivation (tail) currents via non-inactivating Ca channels. With this current blocked, the remaining transient had properties of charge movement (ON-OFF equality, saturation, voltage-dependence of kinetics). This charge had the following average Boltzmann parameters (7 fibers): Q_{max} = 46 nC/μF, $\bar{V}$ = -108 mV, K = 19 mV. Charge movement in a non-polarized fiber (charge 2) thus seems much more steeply voltage dependent than previously reported. Linear capacitive charge was measured with positive pulses from a holding potential of 0 mV; nonlinear charge in the normally polarized fibers had average parameters: Q_{max} = 44 nC/μF, $\bar{V}$ = -54 mV, K = 27 mV. Little charge moved in the voltage range of charge 2. Charge 2 thus seems to convert to charge 1 when the fiber is polarized. These results are similar to recently reported properties of the Na gating currents of squid axon (Bezanilla et al, 1982). They are explained assuming that prolonged depolarization puts the voltage sensor of E-C coupling in a subset of inactivated states in which the system can undergo charge-moving transitions that do not elicit Ca release. Supported by NIH grant AM32808.

M-AM-C4 E-C COUPLING EFFECTS OF INTERVENTIONS THAT REDUCE SLOW Ca CURRENT SUGGEST A ROLE OF T-TUBULE Ca CHANNELS IN SKELETAL MUSCLE FUNCTION. E. Rios, G. Brum and E. Stefani*, (introduced by C. Schauf). Department of Physiology, Rush Medical School, Chicago, and * Centro de Investigacion del IPN, Mexico.

Several interventions that reduce current through the 'slow' t-tubule Ca channel were observed to inhibit EC coupling in voltage-clamped cut segments of skeletal fibers of the frog. Changes in myoplasmic $[Ca^{2+}]$ (Ca transients) were determined with Antipyrylazo III and Ca release flux was derived from the Ca transients. Charge movements were determined as in the preceeding communication. Low external $[Ca^{2+}]$, extracellular Cd^{2+} (3 mM) and nifedipine (15 µM) reduced or eliminated Ca release flux. Nifedipine and low $[Ca^{2+}]_e$ applied together reduced the amount of charge that moved in the voltage range of charge 1 and increased the amount moving in the range of charge 2. Hyperpolarization to -140 mV reversed this effect.

It has been shown that: (a) the specific dihydropyridine binding sites of muscle have a single K_D (Fosset et al, 1984); (b) binding of dihydropyridines (Schwartz et al, 1985) and block by them (Bean, 1984) are voltage-dependent; (c) the receptor also interacts with D600 (Fosset, et al); (d) D600 has actions on EC coupling (Eisenberg et al, 1983; Hui et al, 1984; Lüttgau, unpublished); (e) mice with muscular dysgenesis lack EC coupling, they also have fewer nitrendipine receptors (Pincon-Raymond et al, 1984) and lack slow Ca currents (Beam et al, 1985). A hypothesis explains all of the above results: that the voltage sensing device of EC coupling is also a Ca channel or a closely related molecule that carries the dihydropyridine binding site. Consequently, intramembrane charge movement would be the gating current of this Ca channel.

M-AM-C5 DEVELOPMENTAL INCREASE IN SKELETAL MUSCLE SLOW CALCIUM CURRENT. C.M. Knudson, S.D. Jay & K.G. Beam. Dept. Physiol. & Biophys., Univ. of Iowa, Iowa City, IA 52242

A slow Ca current (I_{slow}) is present in adult skeletal muscle fibers, but its function remains obscure: the Ca to activate contraction is provided by the SR rather than by entry from the extracellular space. One possibility is that I_{slow} is vestigial in adult muscle and physiologically significant only in developing muscle. To investigate this we used the whole-cell patch clamp to measure Ca currents and voltage-dependent charge movements in dissociated fibers of the FDB muscle from 0-50 day old rats. As we have previously described (Neurosci. Abstr. 11:792) two Ca currents are present in fibers of neonatal (<14d) rats: I_{slow} is a maintained current elicited by test pulses > 0 mV; depolarizations of -40 to 0 mV selectively activate a transient current, I_{fast}. Blocking both currents with 1 mM Cd did not prevent contractile responses to brief electrical stimuli or to focal application of 300 mM KCl. Thus, even in neonatal muscle, the entry of external Ca does not appear to have a causal role in E-C coupling. The relative magnitudes of the two currents change with development. In fibers from 0-5 day animals, the peak I_{fast} averaged 3.9 ± 1.8 pA/pF (mean ± sem, normalized by linear cell capacitance) and the peak I_{slow} 5.3 ± 1.1 pA/pF. In fibers from older animals (25-50 d) I_{fast} is too small to be detected, whereas I_{slow} has increased to 18.8 + 3.5 pA/pF. Over this same time span the quantity of charge movement increases from about 6 to 25 nC/uF. The postnatal increase in peak I_{slow} is the opposite of what one might expect for a vestigial membrane protein. Thus, even though Ca entry via I_{slow} does not appear to function in E-C coupling, the channel protein seems likely to be important to the function of adult muscle.

M-AM-C6 CONTRACTURE OF SKINNED SKELETAL MUSCLE FIBERS INDUCED BY IONIC SUBSTITUTION: COMPARISON OF BLOCK BY D-600 AND NITRENDIPINE. Michael D. Fill and Philip M. Best, Department of Physiology and Biophysics, University of Illinois, Urbana, IL 61801.

The ability of D-600 and nitrendipine to block contractures in mechanically inactivated and fully reprimed skinned muscle fibers was investigated. Single fibers from Semitendinosus muscles were skinned (sarcolemma removed manually) and then stimulated by ionic substitution; K propionate was replaced with choline chloride in the bathing solution (constant K x Cl product). Solutions contained in millimoles per liter: 125 monovalent cation, 2 MgATP, 1 Mg, 5 creatine phosphate, 0.5 EGTA (pCa=7.3), and approximately 30 MOPS buffer (pH=7 at 20°C) to make I=0.15. Immediately following a contracture fibers enter a refractory (inactivated) state and must recover (reprime) before another contracture can be elicited. Reprimed and mechanically inactivated fibers were exposed to 10 µM D-600. D-600 block of mechanically inactivated fibers was rapid, while fully reprimed fibers showed little drug effect after two minutes. When exposed to 10 µM nitrendipine, fully reprimed fibers showed a time-dependent block of contracture with 50% block at 30 seconds and complete block after 2 minutes. If mechanically inactivated fibers were allowed to reprime in the presence of nitrendipine, the degree of block at any time during recovery was the same as that of fully reprimed fibers exposed to drug for the same length of time. This suggests that the extent of nitrendipine block is independent of the degree of mechanical inactivation. In contrast, fibers are most susceptible to D-600 block when they are in the mechanically inactivated state. Supported by NIH AM32062 and PHS training grant 5-P32GM07283.

M-AM-C7 ACTIVATION OF CONTRACTION BY NA/CA EXCHANGE IN ISOLATED FROG HEART CELLS. N. Shepherd and W. Spielman, Downstate Medical Center, Brooklyn, NY (Intr. by W. Hurlbut)

We have attempted to assess the relative importance Ca^{++}-channels and Na/Ca exchange to E-C coupling in collegenase-dissociated, single atrial and ventricular cells of Bullfrog heart. We applied pulses of cadmium (1 to 1000 uM) to cells between and during electrically driven twitch contractions and current-induced contractions (3-5 sec. duration), and observed the effects on force development. Force measurements were made with an isometric transducer and the superfusate could be 90% exchanged within 50 ms. With extracellular calcium at 2 mM, 1 uM Cd^{++} reduced peak twitch force to 60% of control, though 17% of control force remained in 100 uM Cd^{++} and 8% in 1 mM. The $[Cd^{++}]$-force relation could be described by assuming two sources of activator calcium, one blocked by micromolar cadmium and contributing about 60% of the calcium, the remainder being blocked by millimolar Cd^{++}. All force development was abolished by removal of extracellular Ca^{++}. 50 ms. pulses of 1 uM - 100 uM Cd^{++} depressed peak force when applied in the early rising phase of the contraction but not at later times, as expected for the blockade of a voltage-dependent calcium channel. To the contrary, plateau force of contractures was not reduced, and sometimes was potentiated, by $[Cd^{++}]$ less than 100 uM. Catecholamines are known to potentiate phasic contractions and depress tonic contractions in frog atrium. Levarteranol (1 ug/ml) was found to abolish contraction (twitch) in the presence of 100 uM Cd^{++} and to cause a sudden decrease and slow increase of twitch force in the absence of Cd^{++}. Activation of twitch contractions in frog heart thus depends on entry of outside Ca^{++} by two means: a Ca^{++} channel and a mechanism like that underlying the tonic contractions observed in other frog heart preparations, probably a Na/Ca exchange.

M-AM-C8 CALCIUM EXCHANGE IN CULTURED MYOCARDIAL CELLS: DETECTION OF INTRACELLULAR COMPARTMENTS Janis M. Burt, Department of Physiology, University of Arizona, Tucson, AZ 85724.

It was reported (GA Langer et al, Am J Physiol 237:H239-H246) that in the absence of proton-donating anions extracellular calcium enters cultured neonatal rat myocardial cells, supports contraction of the myofilaments, and leaves the cell without entering intracellular compartments such as the sarcoplasmic reticulum (SR) or mitochondria. The implication of this observation is that the mitochondria and SR are not involved in excitation-contraction coupling under these conditions. I have reexamined this issue. Cells were incubated in balanced saline solution buffered with N-2-hydroxyethylpiperazine-N'-2-ethanesulfonic acid (HEPES-BSS) containing ^{45}Ca (5 mCi/mmole Ca; a specific activity five times that used in previous studies) for varying periods of time at 24-25°C. Efflux was then studied using the scintillator-disc flow-cell technique. Uptake was dependent on the duration of the labelling period. Half time for labelling was approximately 8 minutes. Uptake is also dependent on the pH of the uptake solution, with an increase in net uptake of approximately 15% at pH 7.6 vs. 7.0. Efflux is enhanced by alkaline pH, the rate constant shifting from -0.0150 min^{-1} at pH 7.0 to -0.0257 min^{-1} at pH 7.6. Efflux is slowed by 47% by 10 mM caffeine an inhibitor of SR function (-0.0193 to -0.0102 min^{-1}), by 15% by 0.05 mM warfarin an inhibitor of mitochondrial function (-0.020 to -0.0169 min^{-1}), and by 60% by 1.0 mM La^{3+}. These data are similar to data collected in the presence of proton-donating anions (GA Langer et al, J Mol Cell Cardiol 15: 459-473) and are indicative of participation of intracellular organelles in the exchange pattern for these cells and in excitation-contraction coupling while perfused with HEPES-BSS. Failure to detect the activity of these compartments in previous studies probably reflects inability of the equipment to differentiate the cell associated isotope from background. This was overcome in these experiments through use of a higher specific activity (5 vs. 1 mCi/mmole Ca) during the labelling period. Supported by NIH HL31008, the Arizona Chapter of the American Heart Association, and the Flinn Foundation.

M-AM-C9 CYTOSOLIC FREE Ca^{2+} LEVELS IN DISSOCIATED ARTERIAL SMOOTH MUSCLE CELLS IN SUSPENSION: CORRELATION WITH CONTRACTION. D. Ashen, W.F. Goldman, T. Ashida and M.P. Blaustein, Dept of Physiol., Univ. of Maryland Sch. Med., Baltimore, MD, 21201.

The normal trigger for contraction of arterial smooth muscle (ASM) is an increase in the cytosolic free Ca^{2+} concentration, $[Ca^{2+}]_i$. Nevertheless, $[Ca^{2+}]_i$ has not previously been measured in living arterial cells. We used the highly fluorescent, Ca^{2+}-sensitive dye, fura-2, to measure $[Ca^{2+}]_i$ in suspensions of dissociated ASM cells under resting conditions and during activation with norepinephrine (NE). ASM cells were dissociated from bovine tail arteries by enzymatic digestion. The cells appeared spindle-shaped, and contracted in response to NE. The cells were loaded with fura-2/AM (2 μM), washed, and suspended in Kreb's solution (33°C) containing 1.0 mM Ca^{2+}. Fura-2 fluorescence was measured with a spectrofluorometer set at 340 and 380 nm for excitation and 510 nm for emission. The resting $[Ca^{2+}]_i$ was 164 $\pm$ 43 nM (n=8). When NE was added to the incubation medium (10^{-6} M final concentration), $[Ca^{2+}]_i$ increased to 305 $\pm$ 59 nM (n=4) during the first minute. Thereafter, $[Ca^{2+}]_i$ continued to increase, but at a slower rate; after 5 min, a level of 462 $\pm$ 157 nM (n=4) was attained. Fura-2 fluorescence did not change during a 7-10 min incubation at 33°C in the absence of NE. Also, the alpha-antagonist phentolamine (10^{-6} M) attenuated the response to 10^{-7} M NE. The time course of the NE-induced changes in $[Ca^{2+}]_i$ corresponded to the time course of contraction of "intact" rings of bovine tail artery: the rings exhibited a rapid initial contraction, followed by a slower rise in tension over several minutes. These results indicate that (1) dissociated ASM cells retain functional integrity, and (2) fura-2 can be used to determine $[Ca^{2+}]_i$ in suspensions of resting and activated dissociated ASM cells. Supported by NIH & AHA.

M-AM-C10 SARCOLEMMAL Ca BINDING AS A MODIFIER OF CARDIAC MUSCLE CONTRACTION. Donald M. Bers, Lee Ann Allen and Youngjee Kim. Div. Biomed. Sci., Univ. of California, Riverside, CA 92521.

Passive Ca binding to rabbit cardiac sarcolemmal (SL) vesicles was measured under ionic conditions similar to extracellular and intracellular media. SL Ca binding in extracellular medium was measured ± ouabain, verapamil, nifedipine, Bay K 8644, caffeine, ryanodine and milrinone over a range of concentrations at which these agents exert strong effects on cardiac contractile performance. None of these agents produced significant alterations in Ca binding such that no part of their actions can be attributed to changes in Ca binding to the external SL surface. In contrast, when half of the 140 mM Na is replaced isosmotically, SL Ca binding increases (e.g. with sucrose, Tris, choline) or decreases (with Li or Cs) depending upon what replacement is used. Thus, the possible effect of Na reduction on surface Ca must be considered in physiological experiments where extracellular [Na] is changed. The effects of membrane potential, [Na] and [Mg] on Ca bound to the SL was measured under ionic conditions similar to those expected intracellularly (e.g. [Ca] = 0.3 to 5 μM). Ca binding was inhibited by physiological concentrations of Na and Mg and was sensitive to membrane potential such that depolarization of a normally polarized cell would cause Ca to be released from these SL sites. Quantitatively, it is not clear whether the effect of depolarization would be to contribute SL bound Ca to the activation of the myofilaments or merely to limit the ability of the inner SL surface to buffer the rise in intracellular [Ca] associated with contraction.
(Supported by NIH HL30077 and Amer. Heart Assoc. & Calif. Affiliate)

M-AM-C11 EFFECTS OF REST AND RYANODINE ON EXTRACELLULAR Ca CHANGES MEASURED BY Ca-SENSITIVE MICROELECTRODES IN RABBIT VENTRICULAR MUSCLE. Kenneth T. MacLeod & Donald M. Bers, Div. Biomed. Sci., Univ. Calif., Riverside, CA 92521.

Cumulative depletions of extracellular Ca, measured using double barreled Ca-sensitive microelectrodes, were produced by 1 Hz stimulation after 10 sec - 10 min. of rest. Depletion size increased while the first post-rest contraction decreased with increasing rest. The depletions may represent refilling of SR Ca stores which have become depleted of Ca during the rest interval. The longer the rest duration the lower the SR Ca content, so the SR is then capable of taking up larger amounts of Ca. This may be related to the rest decay of tension of the first post-rest beat since this is thought to be SR dependent. Ryanodine (1μM) increased the size of the depletions after short rest intervals (< 2 min) but not after longer (≥ 2 min) intervals. Ryanodine increased the rate of Ca efflux from the cell on cessation of stimulation. This may allow the SR to take up more Ca than untreated muscles during subsequent stimulation, thus cumulative depletions are enhanced. When a Ca load was produced during quiescence (0 Na_o) or continuous stimulation (3 μM acetylstrophanthidin), addition of ryanodine (5-10 μM) did not produce any apparent Ca efflux. Caffeine (10mM), added after ryanodine, induced contractures accompanied by Ca efflux implying there was Ca in the SR after ryanodine exposure. Ryanodine appears to enhance Ca efflux upon cessation of stimulation but not during continuous stimulation or quiescence. (Supported by NIH HL30077 and the American Heart Association National and Californian Affiliates).

M-AM-C12 RYANODINE BLOCKADE OF CALCIUM-INDUCED CALCIUM RELEASE FROM THE SARCOPLASMIC RETICULUM IN RAT CARDIAC MYOCYTES IS "USE-DEPENDENT." Michael D. Stern, Don J. Pelto, Maurizio C. Capogrossi and Edward G. Lakatta (Intr. by G. Gerstenblith). Johns Hopkins Medical Institutions and Gerontology Research Center, National Institute on Aging, Baltimore, MD

Ryanodine (RY), which produces a marked negative inotropic effect in rat cardiac muscles, and converts their normal twitch rest potentiation (RP) into rest decay (RD), is believed to act by producing prolonged blockade of the Ca^{2+} release channel of the sarcoplasmic reticulum (SR). In isolated SR fractions, selective binding of RY has an absolute requirement for >6 μM Ca^{2+} (Fed. Proc. 44:1229, 1985). If this requirement exists in the intact cell, RY should act only during the twitch or during spontaneous contractile waves due to Ca^{2+} release from the SR (without sarcolemmal depolarization), since these are the only occasions when $[Ca^{2+}]_i$ reaches micromolar levels (J. Gen. Physiol. 85:189, 1985). To look for Ca^{2+} dependence of RY action, Ca^{2+}-tolerant rat ventricular myocytes were field stimulated at 1 Hz in $[Ca^{2+}]_e$ = 1.5 mM before and after 15 minute exposure to RY 100 nM; extent of shortening was measured by video edge tracking (Figure). Prior to RY, all cells exhibited RP. Cells which were stimulated during RY exposure, and unstimulated cells in which spontaneous contractions were provoked by raising $[Ca^{2+}]_e$ during RY exposure developed RD characteristic of RY effect. In contrast, cells which were maintained quiescent in 0.2 mM Ca^{2+} during RY still exhibited RP after RY. We conclude that RY blockade of SR Ca^{2+} release is use-dependent and that intracellular Ca^{2+} rise, rather than sarcolemmal depolarization, is the mediator of RY use-dependence.

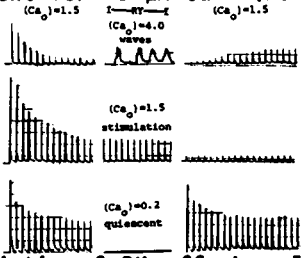

M-AM-D1 INTERACTION FORCES UNDERLYING MEMBRANE FUSION. S. Ohki, Dept. of Biophysical Sciences, State University of New York at Buffalo, Buffalo, N.Y. 14214

Physical basis for a general theory of membrane fusion is given in terms of molecular interaction energy, where the two interacting membranes are considered as two identical flat hydrocarbon plates of infinite thickness having hydrophilic polar layers on their surfaces, separated by a medium at a short distance.

The van der Waals attractive interaction energy between the two plats at a given separation distance plays a decisive role in membrane fusion, which depends upon the nature(interaction coefficient) of the surface hydrophilic layers and their thicknesses. When the surface hydrophilic layer becomes sufficiently similar to the bulk hydrocarbon plates in nature or the thickness of the hydrophilic surface layer becomes small enough, which is related to the interfacial tension of the membrane surface, the attractive interaction energy becomes large and the two plates in close contact could fuse and become one.

The recent studies on phospholipid membrane fusion are discussed in connection with the theory proposed. (supported by a grant fron the U.S. National Institutes of Health (GM 24840).

M-AM-D2 STABILIZATION OF LIPID BILAYER VESICLES BY SUCROSE DURING FREEZING. G. Strauss and H. Hauser, Laboratory for Biochemistry, Eidgenössische Technische Hochschule, Zürich, Switzerland.

The freeze-induced fusion and leakage of small unilamellar vesicles (SUV) formed from natural and synthetic phosphatidyl cholines, and the suppression of these processes were examined. Electron micrographs of SUV suspensions slowly frozen in water showed that the lipid was compressed between ice crystals into a small interstitial volume, and transformed into multilamellar aggregates without any vesicular structure. When frozen in 10% sucrose solution the lipid was also compressed between ice crystals, but remained as SUV. The fraction of lipid remaining as SUV after freezing was measured by turbidity and by high resolution ^1H NMR methods. The %age of SUV recovered increased significantly only at sucrose:lipid mole ratios above 0.4. Eu^{3+} ions abolished the protective effect of sucrose, suggesting that sucrose binds to vesicles, most likely to the phosphate group. ESR studies showed that fusion of vesicles without sucrose is far more extensive if the suspension freezes while the lipid is above its phase transition temperature (T_c) than if freezing occurs while the lipid is below its T_c. ESR spectra of various spin probes incorporated into vesicles showed that the bilayer interfacial region in water retains some mobility down to -50°C. With sucrose this mobility was already lost at somewhat higher temperatures. It is concluded that sucrose exerts its cryoprotective effect by binding to the bilayer interface. Additionally it may create a sucrose-water matrix at low temperatures which prevents vesicles being deformed and ruptured.

M-AM-D3 MEMBRANE CONTACT, FUSION AND HEXAGONAL (H_{II}) TRANSITION IN PHOSPHATIDYLETHANOLAMINE (PE) LIPOSOMES. T.M. Allen and D. Papahadjopoulos. Cancer Research Institute, University of California, San Francisco and Department of Pharmacology, University of Alberta, Edmonton.

The behaviour of egg PE (EPE) and transesterified PE (TPE) in small and large unilamellar and multilamellar liposomes (SUV, LUV and MLV) has been studied as a function of temperature, pH, ionic strength and divalent cation concentration by differential scanning calorimetry (DSC), light scattering (LS), by assays determining liposomal lipid mixing (LM) and content mixing (CM), and by liposomal content leakage (CL) assays. The H_{II} phase transition for EPE and TPE was evident at 42°C and 64°C, and the main (solid-liquid crystalline) transition (T_c) was at 9°C and 15°C, respectively, at pH 7.4 by DSC. The H_{II} transition temperature (TH_{II}) increased and the enthalpy decreased as the pH was raised, and disappeared above pH 8.3 where PE becomes net negatively charged. No changes in LS, LM, CL or CM could be observed at TH_{II} at either low or high pH at low ionic strength (5 mM Na^+). However, when aggregation was induced by addition of Ca^{++} or Mg^{++} (or by increase in [Na^+] to 100 mM, below 8.3), increases in LS, CL and CM occurred at TH_{II}, but fusion (CM) also was apparent between T_c and TH_{II}. We conclude that fusion of PE liposomes below TH_{II} can be triggered by H^+, Na^+, Ca^{++} or Mg^{++} under conditions that induce membrane contact. There was no evidence of the participation of H_{II} transitions in these fusion events.

[Supported by AHFMR, MCR (MA-6487) and NIH (GM28117)].

M-AM-D4 MEMBRANE FUSION, ISOTROPIC INTERMEDIATES AND THE $L\alpha$ -H_{II} PHASE TRANSITION.
Joe Bentz,[a] Harma Ellens,[a] Francis C. Szoka,[a] Joel Oliver[b] and Dave Siegel[b]. [a]Departments of Pharmacy and Pharmaceutical Chemistry, University of California, San Francisco CA 94143 and [b]Proctor & Gamble Co., P.O. Box 39175, Cincinnati, OH 45247.

We have found for several types of PE (phosphatidylethanolamine) containing liposomes that there is a direct correlation between liposome fusion (mixing of aqueous contents) and the existence of a well known, but little understood, hysteretic intermediate state between the lamellar L_α and the hexagonal H_{II} phase. In the past, this state has been characterized by cubic X-ray diffraction patterns, isotropic ^{31}P-NMR signals and/or lipidic particles/interbilayer attachment sites using freeze fracture electron microscopy. We find that DOPE/CHEMS (cholesterylhemisuccinate) liposomes in the presence of Mg^{2+} show enhanced fusion in a temperature range wherein a cubic x-ray diffraction pattern is seen. In Ellens et al. (this volume), N-methyl- DOPE liposomes at pH 7.4 are shown to undergo fusion only within the temperature range, denoted T_I, wherein an isotropic ^{31}P-NMR signal is found by Gagné et al. (1985) Biochemistry, in press. Above T_I, at the temperature range of the pure H_{II} phase, denoted T_H, the liposomes undergoes a contact mediated lysis, as we have shown previously with other polymorphic lipid mixtures (Bentz et al. (1985) Proc. Natl. Acad. Sci. 82, 5742; Ellens et al. (1985) Biochemistry, in press). From these results and theoretical calculations, we have derived a molecular mechanism which can explain both the liposome fusion and the more general problem of the L_α - H_{II} phase transition. Supported by NIH Grants GM-31506 (J.B.) and GM-29514 (F.C.S.)

M-AM-D5 LECTIN-MEDIATED AGGLUTINATION AND FUSION OF GLYCOLIPID/PHOSPHOLIPID VESICLES: EFFECT OF CARBOHYDRATE HEAD-GROUP SIZE, CALCIUM IONS AND SPERMINE. D. Hoekstra and N. Düzgüneş, Lab. of Physiological Chemistry, Univ. of Groningen, 9712 KZ Groningen, The Netherlands, and Cancer Research Institute and Dept. of Pharmaceutical Chemistry, Univ. of California, San Francisco, CA 94143

We have studied the susceptibility of liposomes containing various glycolipids to Ricinus communis agglutinin(I)-induced agglutination, and Ca^{2+}- and spermine-induced aggregation and fusion in the presence or absence of the lectin. The liposomes were composed of phosphatidylethanolamine, phosphatidic acid and either galactosyl cerebroside (GC), lactosylceramide (LC), or trihexoside ceramide (TC) at a molar ratio of 3.5:1.0:0.45. The initial rates of agglutination increased in the order GC<<LC<TC, while a reversed order was obtained for Ca^{2+}- and spermine-induced aggregation and fusion, indicating an enhanced steric hindrance to close approach of bilayers with increasing head-group size. Lectin-mediated agglutination rates for LC- and TC-vesicles increased by an order of magnitude in the presence of Ca^{2+} at a concentration which did not itself induce aggregation. Charge neutralization could not account for this observation, as spermine did not display this synergistic effect. The threshold Ca^{2+} concentration for fusion was reduced from mM to uM when the vesicles were pre-agglutinated, and decreased with carbohydrate head-group size. The distinct effects of Ca^{2+} and spermine on lectin-induced agglutination on the one hand and fusion on the other, could be due to the regulation by Ca^{2+} of the steric orientation of the carbohydrate head-group, which appears to be related to the ability of Ca^{2+} to dehydrate the bilayer.

Supported by NIH Grant GM28117, NATO Research Grant 151.81 and an AHA Grant-in-Aid.

M-AM-D6 pH-DEPENDENT LYSIS OF LIPOSOMES BY ADENOVIRUS: A MODEL FOR ENTRY INTO THE CYTOPLASM.
Robert Blumenthal, Prem Seth, Mark Willingham and Ira Pastan NCI, NIH, Bethesda, MD 20892

Adenovirus is a non-enveloped virus whose nucleocapsid finds its way to the cytoplasm of the host cell by receptor-mediated endocytosis, followed by disruption of the the membrane of the endocytic vesicle. In order to examine the mechanism of this membrane disruption we studied the interaction of adenovirus with liposomes. Purified adenovirus induced a dose-dependent release of the water-soluble marker calcein from liposomes. Marker release was strongly dependent on pH, and at temperatures below 5°C the rate of release showed an optimum at a pH of about 6. This pH-dependence parallels disruption of endocytic vesicles by adenovirus, and the permeabilization that adenovirus induces on the cell surface. The rate of release at pH 6.1 and 2°C showed the following lipid dependence of the target membrane: Egg PC:Chol (1.5:1) > Egg PC:PS (1:1) > Egg PC >>> DPPC. At temperatures above 5°C adenovirus-induced release at the lower pH was reversibly inhibited due to virus-virus interaction. Binding of virus to liposomes showed a similar pH-dependence as release, but was not temperature-sensitive. "Non-specific" binding of virus to liposomes could be inhibited by preincubation in 30% glycerol or 0.6 M sucrose. Dilution of the mixture into a glycerol or sucrose-free medium resulted in an instantaneous pH-dependent release of marker at 23°C. Using the self-quenching properties of calcein we show that adenovirus-induced marker release from individual liposomes was graded rather than all-or-none. Electron microscopy using negative stain showed liposomes bound to adenovirus. In some cases, the liposomes were still intact, but many liposomes, which were attached to the vertices of the virus, appeared lysed.

M-AM-D7 QUANTAL NATURE OF THE CALCIUM-DEPENDENT, ACETYLCHOLINE-EVOKED ATP RELEASE FROM ADRENAL CHROMAFFIN CELLS. Eduardo Rojas and Harvey B. Pollard, LBC & G, NIH, Bethesda, MD 20205

Adrenal chromaffin cells secrete catecholamines and ATP stored in secretory granules, and the release process can be measured in real-time by including luciferin-luciferase in the incubation physiological external medium. In response to acetylcholine at 36 °C, ATP release from cells followed a double exponential time course with extrapolated initial rates of 0.005 and 0.0017 % total ATP in the cells per second and rate constants of 0.08 and 0.013 s^{-1} respectively. The activation energy, estimated from the effects of temperature on ATP release, was similar for both processes, about 18 kcal $mole^{-1}degree^{-1}$ respectively. Fluctuation analysis of the light signal was used to obtain information on the microscopic characteristics of the release process. At 18 °C, the excess noise of the acetylcholine-evoked increase in light, after subtracting the contributions from the photomultiplier and the luciferin-luciferase reaction from the total, could be described in terms of a single Lorentzian power spectrum with a corner frequency near 10 Hz. Increasing the temperature to 36 °C increased the corner frequency to 25 Hz. At this temperature, a second Lorentzian could be resolved with a corner frequency of 90 Hz. As the time course of the light glow due to the ATP discharge from a single granule at the site of exocytosis is complex, the size of the unitary events could not be obtained directly from the variance. However, assuming an exponential decay of the unitary event (time constant = 16 ms), the frequency of events causing the measured variance is estimated in the order of 10^4 s^{-1}. Thus, this assay allows us to measure stimulated secretion from chromaffin cells with a time resolution in the millisecond range and to examine single exocytotic events.

M-AM-D8 SYNEXIN-INDUCED FUSION OF CHROMAFFIN GRANULE GHOSTS (CGG) STUDIED BY A NOVEL FLUORESCENCE ASSAY. Andres Stutzin and Harvey B. Pollard. Laboratory of Cell Biology and Genetics, NIADDK, NIH, Bethesda, MD. 20205.

Membrane fusion is a crucial step in various biological processes including fertilization, exocytosis and neurotransmission, and may be regulated by intracellular proteins, such as synexin, a calcium-binding protein found in the adrenal medulla and other secretory tissues. In order to study the role of synexin in fusion of biological membranes, a novel on-line fluorescence assay was devised. Fluorescein-isothyocianate conjugated to dextran (MW 20,000) was trapped within CGG at self-quenching concentrations and fusion detected by relief of self-quenching when loaded ghosts were mixed with empty vesicles. An anti-fluorescein antibody in the medium quenched free fluorescein released by simple leakage. Under these conditions, purified synexin triggered a change in the fluorescence output due to mixing of the aqueous contents of the vesicles (i.e. fusion). This fusion process occurred over several minutes and could be resolved into a fast initial phase and a slow, second one. Fusion was dependent on the concentration of synexin, pH and temperature and was calcium independent in the range of 10 nM to 10 mM free calcium concentration. However, the fusion was strongly inhibited by a specific anti-synexin polyclonal antibody. By contrast, heat-denatured synexin, as well as non-related proteins such as bovine serum albumin, were unable to elicit fusion. Trypsin treatment as well as exposure of the granule membranes to an impermeant carbodiimide, which modifies carboxyl groups, inhibited the fusion reaction to different extent. These results suggest that synexin can support specific fusion mechanisms independent of calcium, and these data may lend insight into fundamental fusion processes in vivo.

M-AM-D9 A MODEL FOR FUSION BASED ON THE OPENING OF CALCIUM-ACTIVATED POTASSIUM CHANNELS. G. Ehrenstein and E. Stanley, Lab. of Biophysics, NINCDS, NIH, Bethesda, MD 20892.

It is well known that an increase in cytoplasmic calcium concentration stimulates the fusion of vesicles with the plasma membrane and that this leads to the secretion of hormones and neurotransmitters. We hypothesize that vesicle membranes contain calcium-activated potassium channels and that the chief function of the increased cytoplasmic calcium is to open these channels. The opening of these cationic channels coupled with anion transport across the vesicle membrane would result in an increase of osmotic pressure in the vesicle. Some vesicles situated very close to the cell plasma membrane would reach the osmolarity threshold required for fusion with the membrane. This would result in secretion of the vesicle contents. For other vesicles that do not fuse, some of the increased osmolarity would be retained between action potentials, thus lowering the incremental increase in osmolarity required for fusion. This would be observed as facilitation. This model can account for many known properties of transmitter release, including:

1) the high specificity for calcium over other divalent cations
2) the brief interval between the entrance of calcium into a terminal and transmitter release
3) the dependence of transmitter release on the fourth power of calcium concentration
4) the dependence of facilitation on the stimulus frequency

M-AM-D10 EVIDENCE FOR CALCIUM-ACTIVATED POTASSIUM CHANNELS IN VESICLES OF PITUITARY CELLS. E. Stanley*, G. Ehrenstein*, and J. Russell#, NIH, Bethesda, MD 20892. *Lab. of Biophysics, NINCDS; #Lab. of Neurochemistry and Neuroimmunology, NICHD.

The model for fusion of vesicles with the cell plasma membrane described in the preceding Abstract hypothesizes that vesicle membranes contain calcium-activated potassium channels. To test this hypothesis, we have attempted to reconstitute the putative channels from vesicles of pituitary cells into lipid bilayers. The bilayers were formed from phospholipids by the brush technique, and vesicles were added to one side of the lipid bilayer. Single channels of small amplitude were observed spontaneously. After the addition of micromolar concentrations of calcium to the side of the membrane that would correspond to the cytoplasm of cells, single channels of about 300 pS were observed. Millimolar barium added to the same side as the calcium blocked the channels. Subsequent addition of a larger concentration of calcium than previously added resulted in the reappearance of channel openings.

The observation of these reconstituted channels supports the model for fusion based on the opening of calcium-activated potassium channels.

M-AM-D11 MECHANISMS OF EARLY EVENTS IN MAGNESIUM- AND CALCIUM-PROMOTED BILAYER MEMBRANE FUSION STUDIED BY AN IMPROVED ASSAY UTILIZING THE MONOMER/EXCIMER FLUORESCENCE RATIO FROM CHAIN-LABELLED PYRENE-PHOSPHATIDYLCHOLINE. Stephen J. Morris, Diane Bradley, Carter C. Gibson* and Paul D. Smith*. Neurotoxicology Section, LENP, NINCDS, and *Biomedical Engineering and Instrumentation Branch, DRS, NIH, Bethesda, MD 20205, USA.

We have investigated chain labelled pyrene-PC as a probe to study the rapid kinetics of membrane fusion. In agreement with Roseman and Thompson [Biochem. 19:439(1980)] and Massey et al [JBC 257:5444(1982)], we find that the spontaneous exchange rate for this probe between PC bilayers is very slow. Similar results were obtained for PS:PE 1:1 bilayers. This slow exchange, in contrast to rapid exchange of chain labelled NBD-PC probably is due to the tremendous increase in hydrophobicity of the pyrene versus the NBD molecule [Nichols and Pagano, Biochem. 21:1720(1982)].

The ratio of monomer to excimer fluorescence (E/M ratio) from pyrene-PC incorporated into PS:PE bilayers is linear with increasing probe concentration up to 6 mol percent probe. Fusion of labelled with unlabelled PS:PE vesicles linearly reduces the E/M ratio as would be predicted by increased distance between fluorophores experienced by fusion. Thus stochastic predictions of extent of fusion can easily be checked experimentally. Stopped-flow mixing experiments show initial Mg^{2+}-promoted fusion of PS:PE vesicles follow second-order, aggregation rate-limited kinetics, as was previously found for Ca^{2+} using the NBD-PE to rhodamine-PE resonance energy transfer assay [Morris, et al, JBC 260: 4122 (1985)]. There is no prolonged or extensive lateral phase separation involved in the calcium- or magnesium-promoted fusion of PS:PE vesicles.

The new assay solves problems encountered in using the NBD-PE/rhodamine-PE assay. NBD-PE fluorescence is shown to be sensitive to changes in the headgroup environment caused by ion binding.

M-AM-D12 PROTON-INDUCED FUSION OF LIPID VESICLES CONTAINING NOVEL pH-SENSITIVE AMPHIPHILES. T. Diacovo, R. Leventis and J.R. Silvius*, Dept. of Biochemistry, McGill University, Montréal, Qué. CANADA H3G 1Y6.

A series of amphiphiles was synthesized with two long alkyl chains and headgroups whose charge varies with pH in the range 4-7. We have examined the proton-induced fusion and destabilization of liposomes composed of these pH-sensitive amphiphiles together with phosphatidylethanolamine (PE), using a combination of fluorimetric assays of vesicle leakage, lipid mixing and contents mixing. Several of the pH-sensitive amphiphiles, notably N-acyl-2-aminopalmitic acid and its amide conjugates with amino acids such as serine and histidine, mediate proton-induced vesicle fusion, including appreciable mixing of contents, at pH values ranging up to 5.5-6.5 when combined with PE in a 3:1 (PE/amphiphile) molar ratio. Fusion of these vesicles can also be induced or enhanced by divalent cations. The structure and physical behavior of these amphiphiles suggests that they may promote controllable fusion of PE-containing vesicles without strongly enhancing the tendency of PE to form the hexagonal II phase. Double-chain pH-sensitive amphiphiles of the types characterized in this study, which can be synthesized conveniently and which should be less prone than single-chain amphiphiles to desorb from vesicles in the presence of cells or serum, may be useful in the design of pH-sensitive liposomes for delivery of encapsulated molecules to cells. (Supported by the Medical Research Council of Canada and the Fonds pour la Formation de Chercheurs et l'aide à la Recherche du Québec).

M-AM-E1 SITE-DIRECTED CHEMISTRY AND SPECTROSCOPY: APPLICATIONS IN THE ASPARTATE RECEPTOR SYSTEM. Joseph J. Falke, David W. Sternberg & Daniel E. Koshland, Jr., Dept. of Biochemistry, University of California, Berkeley, CA USA 94720. Introduced by Tracy Yang.

The bacterial aspartate receptor is a transmembrane protein which transduces environmental stimuli (external aspartate concentration) into an intracellular signal (swimming motor bias), thereby enabling a bacterium to swim up a gradient of aspartate. The transmembrane structure of the aspartate receptor is similar to that of other chemoreceptors, such as the EGF and insulin receptors, suggesting that cell-surface receptors may share a universal mechanism for transmembrane signaling.

In order to understand the conformational changes in the aspartate receptor or any other protein, it is useful to monitor the conformational dynamics at key sites in the protein structure. Site-directed mutagenesis has been used to substitute cysteine residues at 5 important locations in the structure of the aspartate receptor, whose native sequence completely lacks cysteine. These substitutions differ from previous applications of mutagenesis because they are designed to have no effect on the native structure and function of the protein but to serve as sites for chemical modification. All of the mutant receptors have been shown to retain full activity in swarm assays of aspartate-seeking behavior. The mutant receptors contain unique sulfhydryl groups which simplify chemical labeling in sidedness studies and in crosslinking studies of receptor structure. These sulfhydryls also serve as spectroscopic labeling sites which enable unambiguous observation of the conformational dynamics that occur during sensory transduction. The results of these studies will be discussed.

Supported by NIH grant 5 R01 AM09765-21 (DEK) and by an NIH postdoctoral fellowship (JJF).

M-AM-E2 PARTIAL ADAPTATION TO SMALL STIMULI IN THE ABSENCE OF RECEPTOR MODIFICATION, Robert M. Weis & Daniel E. Koshland, Jr. Dept. of Biochemistry, University of California at Berkeley, Berkeley, CA. USA 94720.

Bacterial chemotaxis is a simple behavioral system that allows bacteria to swim toward higher concentrations of attractant and lower concentrations of repellent. Wild type bacteria have the ability to adapt (return to prestimulus behavior) to large changes in attractant or repellent concentration. With an attractant such as aspartate, this is accomplished by reversibly methylating the intracellular portion of a specific membrane receptor protein. The extent of methylation at steady state is proportional to the aspartate concentration. After an increase (decrease) in aspartate concentration, the bacteria respond to this stimulus until the level of methylation increases (decreases) to match the new aspartate concentration.

However it has been observed that bacteria lacking both methylating enzyme and demethylating enzyme activities can respond and partially adapt to small changes in attractant concentration (1,2). The bacteria in the former study (1) were double point mutants (RP447,PS1281). We report now that double deletion mutants in both the methylating and demethylating enzymes (RP1273, RP4969,RP4970) have chemotactic ability similar to the point mutants(10% of wild type), and can respond and partially adapt to small changes (1μM) but not to large changes (>10μM) in attractant concentrations (RP1273). The significance of this adaptation and its implication for information processing in the absence of receptor modification will be discussed.

This work was supported by NIH grant # 5 R01 AM09765-21 to DEK and a Jane Coffin Childs Postdoctoral Fellowship to RMW.

1)Stock, Kersulis & Koshland, Cell 42 (1985) 683-690. 2)Block, Segall & Berg, Cell 31 (1982)215-26

M-AM-E3 AN APPROACH TO LIPID FUNCTION IN AN EXOCYTIC MEMBRANE MICRODOMAIN IN PARAMECIUM Birgit H. Satir and Milaniya Reichman (Intr. by E. Spudich), Department of Anatomy and Structural Biology, Albert Einstein College of Medicine, Bronx, New York.

The exocytic-specific plasma membrane microdomain in Paramecium consists of two rings of intramembrane particles (IMPs) and a central fusion rosette of 9-11 IMPs. A secretory mutant nd9 when grown at 15°C possesses the normal assembled rosette, secretes and dephosphorylates an in vivo stimulus-sensitive phosphoprotein M_r 65Kd in response to trinitrophenol (TNP), but when grown at 27°C lacks the central rosette, does not dephosphorylate the 65Kd protein and does not secrete. The (exo^+) phenotype of nd9 cells depends on temperature-induced changes in lipid composition of the cell membrane (Beisson et al., J. Cell Biol: 85, 1980). We have examined the effect of a fatty acid synthesis inhibitor (cerulenin) on exocytosis and on dephosphorylation in wt and mutant cells. Wt or nd9 cells, grown to stationary phase at 27°C or at 15°C or shifted at stationary phase from 27°C to 15°C were exposed to cerulenin for 18-24h before sampling. In phosphorylation experiments, cells were harvested, incubated for 1h with ^{32}P-labeled phosphoric acid and then stimulated with TNP. SDS-PAGE gels of the total sample were run, followed by autoradiography to determine the state of phosphorylation of the 65Kd protein. In the continued presence of cerulenin, dephosphorylation of the 65Kd protein is inhibited in all wt cultures. The secretory response of these cells determined by light microscopy was also reduced in all conditions tested. Thus, the exo^-phenotype can be reconstituted at any growth temperature in wt cells in the presence of cerulenin. These data suggest that specific lipo-protein interactions at the exocytic membrane microdomain are important and strengthen the correlation between dephosphorylation of the 65Kd protein and exocytosis. Supported by grants from NIH and NCI.

M-AM-E4 REGULATION OF CORTICAL VESICLE EXOCYTOSIS IN SEA URCHIN EGGS BY INOSITOL 1,4,5-TRISPHOSPHATE AND GTP-BINDING PROTEIN. Paul R. Turner[1], Laurinda A. Jaffe[1], and Alan Fein[2]. [1]Dept. of Physiology, University of Connecticut Health Center, Farmington, CT 06032, and [2]Marine Biological Laboratory, Woods Hole, MA 02543.

To investigate the roles of inositol 1,4,5-trisphosphate ($InsP_3$) and guanyl nucleotide binding proteins (G-proteins) in the transduction mechanism coupling fertilization and exocytosis of cortical vesicles in sea urchin eggs, we microinjected $InsP_3$ and guanyl nucleotide analogs into eggs of Lytechinus variegatus. Injection of 28 nM $InsP_3$ caused exocytosis. However, if the egg was first injected with EGTA ($[Ca_i] \leq 0.1$ μM, [EGTA] = 1.6 mM), $InsP_3$ injection did not cause exocytosis, supporting the hypothesis that $InsP_3$ acts by causing a rise in intracellular free calcium. Injection of 28 μM guanosine-5'-O-(3-thiotriphosphate) (GTP-γ-S), a hydrolysis-resistant analog of GTP, caused exocytosis, but exocytosis did not occur if the egg was pre-injected with EGTA. Injection of 3 mM guanosine-5'-O-(2-thiodiphosphate) (GDP-β-S), a metabolically stable analog of GDP, prevented sperm from stimulating exocytosis. However, injection of GDP-β-S did not prevent the stimulation of exocytosis by $InsP_3$. These results suggested the following sequence of events: The sperm activates a G-protein, which stimulates production of $InsP_3$. $InsP_3$ elevates intracellular free calcium, which causes exocytosis. Supported by NIH grants HD14939 to L.A.J., and EY03793 and EY01362 to A.F., and by NIH training grant HD07098 to the Embryology Course at the Marine Biological Laboratory, Woods Hole, MA.

M-AM-E5 OPTICAL MEASUREMENT OF THE BROWNIAN MOTION SPECTRUM OF HAIRBUNDLES IN THE TRANSDUCING HAIR CELLS OF THE FROG AUDITORY SYSTEM. W. Denk and W. W. Webb, Applied Physics, Cornell Univ., Ithaca, NY 14853 and A. J. Hudspeth, University of California School of Medicine, San Francisco, CA.

Differential Interference Contrast (DIC) microscopy with coherent laser illumination and a solid state position sensing quadrant detector allowed us to measure the spectrum of the Brownian motion of the hairbundles protruding from the cells in a vibration detecting organ, the sacculus of the frog rana pipiens (A. J. Hudspeth, Ann. Rev. Neurosci. 6, 187, 1983). Preliminary results suggest a power spectrum of the transverse displacement amplitudes that is flat up to 200 Hz then falls off as $1/f^2$. The observed rms amplitudes lie between 1.5 and 2.5 nm. Thus the equipartition theorem yields a stiffness between 1.8×10^{-3} and 0.6×10^{-3} N/m. So far our results show no indication of active motion. For the necessary fine positioning and calibration we used an x-y stage built of piezoelectric bimorphs (D. P. Corey and A. J. Hudspeth, J. Neurosci. Meth. 3, 183, 1980; D. W. Pohl, W. Denk and M. Lanz, Appl. Phys. Lett. 44, 651, 1984). The use of images formed by a high N.A. (1.25) objective provides sensitivity approaching that achieved by laser interferometer methods (P. R. Dragsten, W. W. Webb, J. A. Paton and R. R. Capranica, Science 185, 55, 1974; P. R. Dragsten, W. W. Webb, J. A. Paton and R. R. Capranica, J. Acoust. Soc. Am. 60, 665, 1976).

Supported by grants from the NSF (DMB 83-03404) and NIH (GM33028) (W.W.W.) and NIH (NS 20429) (A.J.H.).

M-AM-E6 EVIDENCE FOR A ROLE OF VOLTAGE-SENSITIVE POTASSIUM CHANNELS IN TASTE TRANSDUCTION. **S.C. Kinnamon and S.D. Roper (Intr. by M.C. Neville), Rocky Mountain Taste and Smell Center, University of Colorado Health Sciences Center, Denver, CO 80262.**

In previous studies we have shown that mudpuppy taste receptor cells generate action potentials in response to electrical or chemical stimulation. However, the role of voltage-gated conductances in taste transduction remains unclear. In this study, we have examined the role of voltage-sensitive potassium conductance in the transduction of salt (KCl) and sour (citric and hydrochloric acid) taste stimuli into receptor potentials. Taste cells at the normal resting potential (approximately -70 mV) responded with graded depolarizations to focally-applied KCl; the depolarization was accompanied by a slight decrease in input resistance. When the membrane was hyperpolarized to approximately -90 mV (by DC current injection), however, the response to KCl was abolished. Tetraethylammonium bromide (TEA) perfused into the bath caused a reversible 20- 30 mV depolarization of taste cells, accompanied by a large increase in input resistance. TEA completely blocked the KCl-induced depolarization at all membrane potentials. Taste cells at the normal resting potential also responded with graded depolarizations to focally-applied acids; however, the response was prolonged relative to KCl-evoked responses and the depolarization was accompanied by an increase in input resistance. The response to acid was also blocked by TEA or hyperpolarization in excess of -90 mV. We conclude that the "leak" potassium conductance in taste cells is voltage-sensitive, and is the principal conductance involved in KCl taste transduction. In addition, our results suggest that acids produce depolarizing receptor potentials by decreasing this potassium conductance. (Supported by NIH grants NS20382, PO1NS20486-02, and AG03340).

M-AM-E7 DIFFERENT RESPONSES TO SALTS AND SUGARS IN THE ANTERIOR AND POSTERIOR REGIONS OF DOG TONGUE. **S.A. Simon* and J.L. Garvin. *Dept. of Physiology, Duke Univ., Durham, N.C. 27710; L.K.E.M., N.I.H., Bethesda, Md. (Intr. by M. Lieberman).**

Integrated responses from the chorda tympani nerve in dog show that the anterior region of the tongue is more sensitive to salt than the posterior region whereas the opposite is the case for sugars. To determine if the asymmetry is present at the epithelial level, we measured the open circuit potential, Voc, short circuit current, Isc, and specific resistance R_m, from the anterior and posterior regions of the same dog tongue. In symmetric solutions of Krebs-Henseleit (K-H) buffer Voc, Isc and R_m were 10.6mV, -21.6 $\mu A/cm^2$, and 532 Ωcm^2, respectively for the anterior region and were 11mV, -14.5 $\mu A/cm^2$ and 788 Ωcm^2 for the posterior region. In asymmetric solutions, the serosal surface was bathed in K-H buffer whereas the composition of the mucosal surface contained various concentrations of salts and sugars (pH 6-8). For the dose dependent response of Isc and Voc for NaCl, KCl and NH_4Cl (.01 - 0.5M), we found that the change in Voc and K1/2 was similar, but the change in Isc was much higher for the anterior compared to posterior region. For NaCl, ΔIsc= 120 $\mu A/cm^2$, ΔVoc= 20mV, K1/2= ~0.3M for the anterior region while for the posterior region ΔIsc= 80$\mu A/cm^2$, ΔVoc= 22mV, K1/2= ~0.3M. In contrast to the monovalent salts the response to the saccharides, D-glucose, L-glucose, deoxyglucose, fructose and sucrose in 50mM NaCl (to simulate saliva) was found to be greater for the posterior than the anterior regions. For example, for fructose (0 to 0.4M) on the anterior side, ΔIsc= 13 $\mu A/cm^2$, ΔVoc= 16mV and K1/2= 225mM whereas for the posterior region; ΔIsc 18 $\mu A/cm^2$, ΔVoc= 18mV and K1/2= 150mM. These data show that the measured inhomogeneties in the chorda tympani responses are present at the epithelial level, suggesting that events occurring in the epithelium are involved in the transduction process.

M-AM-E8 PRESSURE INJECTION OF cGMP MIMICS EXCITATION IN LIMULUS VENTRAL PHOTORECEPTORS, E.C. Johnson and J.E. Lisman, Dept. of Biology, Brandeis Univ., Waltham, MA 02254

cGMP was pressure injected into Limulus ventral photoreceptor and injections were monitored optically. The injection solution consisted of 1 or 10 mM cGMP in a carrier solution of .3M KAsp, 10mM HEPES pH 7.0. These cGMP injections resulted in rapid depolarizations that were observed only when the pipette was in an unidentified sub-region of the light sensitive lobe of the photoreceptor. The amplitude of the depolarization varied smoothly with the strength of the pressure pulse. When the cGMP injection was large enough to give a 20 to 30mV depolarization, the response saturated and stronger pressure pulses of cGMP resulted only in increasing the response duration. Once the return to baseline began, all responses had a rapid (about 100ms) decay to baseline. Under the conditions studied, cGMP injection did not adapt the light response, nor did light have any noticeable adapting affects on the response to a cGMP injection. Under voltage clamp, the cGMP injection caused an inward current at negative holding potentials. This cGMP induced current had a reversal potential and IV characteristics similar to that of the light induced current. Experiments with double-barrel microelectrodes, in which cGMP was in one barrel and a control solution in the other, demonstrate that both cGMP and its slowly hydrolyzable analog, 8-Br-cGMP, give the response described above, while injections of carrier solution, cAMP, and 5'-GMP have no effect. These results are consistent with cGMP being involved in mediating the light response of invertebrate photoreceptors. (Supported by NIH EY01496 and EY05802).

M-AM-E9 REVERSIBLE ADSORPTION KINETICS ON MEMBRANES MEASURED BY TOTAL INTERNAL REFLECTION FLUORESCENCE. Robert Fulbright and Daniel Axelrod, Dept. of Physics and Biophysics Research Div., University of Michigan, Ann Arbor, MI 48109.

Using variations of total internal reflection (TIR) fluorescence combined with fluorescence photobleaching recovery (FPR), we have examined the surface diffusion and reversible adsorption kinetics of nonspecific binding of fluorescein labeled epidermal growth factor (F-EGF) to human erythrocyte membrane. On cell surfaces containing EGF receptors, these same dynamical properties are relevant to determining the encounter rate between hormone molecules and their receptors. Erythrocyte ghosts were flattened by hemolysis and strong electrostatic attraction to a TIR surface of fused silica coated with a 200 Å thick layer of aluminum and topped by a covalently attached coat of poly-l-lysine. Each ghost thereby splits open and exposes its cytoplasmic and external faces to the solution in clearly distinct regions. Fluorescence of membrane adsorbed F-EGF in equilibrium with free F-EGF in solution was selectively excited by the evanescent wave of a totally internally reflected laser beam. The background fluorescence of F-EGF adsorbed directly to the substrate underlying the erythocyte ghosts was quenched by the prescence of the metal layer, thereby allowing very low concentrations of membrane adsorbed F-EGF to be visualized. Photochemical crosslinking of F-EGF was retarded by enzymatically-aided deoxygenation. Combined with FPR, a spatially uniform TIR illumination of the membrane yielded a membrane membrane residency time for reversibly adsorbed F-EGF of about 0.5 sec. To measure F-EGF surface diffusion, a nonuniform illumination and photobleaching pattern is necessary. For this purpose, we have designed a TIR/FPR system with intersecting laser beams producing interference fringes of less than 1 μm spacing on the membrane.

M-AM-F1 SOME PROPERTIES OF BOUND STATE ELECTRON TRANSFER BETWEEN CYTOCHROME-C AND BACTERIAL PHOTOSYNTHETIC REACTION CENTER. Moser, C. C. and Dutton, P.L.

The kinetics of electron transfer between cyt c and the RC has been described by a model with three states: unassociated RC and cyt c, and two interconvertable bound states, one of which participates in electron transfer with the excited RC (eg. Overfield, R.E. et al.[1] and Dutton et al.[2]). An extension of the analysis to the entire kinetics time course under a variety of conditions for RC solubilized in minimal lauryldimethyamineoxide (LDAO) confirms the three state kinetics model, and reveals two unexpected properties of electron transfer from the bound state. The electron transfer rate from the slower, "distal" bound state, as well as the relative distribution of cyt c between the "distal" and "proximal" bound states, are sensitive to the bulk viscosity ($k = 26\eta/\mu s^{-1} + 75\ \mu s^{-1}$ and $Keq = 0.44\eta + 1.4$, where η is the viscosity relative to water). Second, at relatively low cyt c concentrations cyt c oxidation departs from the theoretical time course due to product inhibition, suggesting that oxidized cyt c effectively competes for the bound sites.
[1] (1980) Biochem. 19, 3322-3327. [2] (1978) in The Photosynthetic Bacteria (Clayton, R.K. et al. eds. 525-570, Plenum Press, N.Y.

M-AM-F2 OXIDATION RATE OF HIGH POTENTIAL CYTOCHROME c_{558} IN REACTION CENTERS FROM Rhodopseudomonas viridis: R.J. Shopes and C.A. Wraight; Univ. of Illinois, Urbana, Il. L.M.A. Levine and D. Holten; Washington Univ., St. Louis, Mo.

The reaction center (RC) from Rps. viridis contains four bound secondary donors; two high potential cyt c_{558} and two low potential cyt c_{553}. When RCs are poised at an E_h of +250mV both high potential cytochromes are able to be oxidized by P^+ in successive turnovers and they have been considered equivalent. The oxidation rate for the high potential cytochrome, measured by an absorption change at 425 nm, has been reported to be $4x10^6\ s^{-1}$, but was coincident with only 40% of the absorption change at 445nm attributed to P^+ reduction [Holten et al. (1978) BBA 501, 112]. The slower change at 445nm, previously assigned to P^+ reduction, was not accompanied by any additional cytochrome oxidation. We have reexamined the absorption change kinetics at a number of wavelengths. The slower ($k \approx 10^5\ s^{-1}$) absorption change exhibits a large bandshift spectrum centered at (about) 420nm, a smaller band shift centered at (about) 558nm and additional features in 750-850nm region. This spectrum is not consistent with the assignment of the slow kinetic to P^+ reduction but is attributable to a transfer, or sharing, of an electron from the initially oxidized cyt c_{558} (c_{HP1}) with the other cyt c_{558} (c_{HP2}). The reaction scheme is:

$$c_{HP2}\ c_{HP1}\ P^+ \xrightarrow{10^6\ s^{-1}} c_{HP2}\ c_{HP1}^+\ P \xrightarrow{10^5\ s^{-1}} c_{HP2}^{1/2+}\ c_{HP1}^{1/2+}\ P$$

This behavior is consistent with the x-ray structure analysis of Rp. viridis RCs [Deisenhofer et al. (1984) J. Mol. Biol 180, 385] which shows all four hemes (low and high potential) in line. This arrangement necessarily renders them all inequivalent. Supported by NSF PCM 83-16487.

M-AM-F3 ELECTRON TRANSFER COMPONENTS OF PHOTOTROPHICALLY AND AEROBICALLY GROWN CHLOROFLEXUS AURANTIACUS. R. Wynn[a], R. Fuller[b], T. Redlinger[b], J. Foster[b], R. Blankenship[c], R. Shaw[a] and D. Knaff[a]. [a]Dept. of Chemistry and Biochemistry, Texas Tech Univ., [b]Dept. of Biochemistry, Univ. of Massachusetts and [c]Dept. of Chemistry, Arizona State Univ.

The gliding green bacterium Chloroflexus aurantiacus possesses the ability for facultative growth. Despite numerous studies on this organism, its electron transfer chain remains largely uncharacterized. Recent studies indicate that the electron transfer chain in Chloroflexus resembles, in some respects, the cyclic chain found in purple phototrophic bacteria. Results from our laboratories indicate the presence of hemes b and c in membranes isolated from aerobic or phototrophic cells. No heme a was detected. Heme c is present in considerable excess over heme b in the membranes from phototrophic cells (c:b = 30:1). In membranes from aerobic cells, this ratio decreases to 3:1. The well characterized, membrane-bound cytochrome c-554 (the donor to the reaction center bacteriochlorophyll in phototrophic cells) is absent in aerobic membranes. EPR measurements indicate the presence of a membrane-bound Rieske iron-sulfur protein. Experiments characterizing possible terminal oxidase(s) in aerobic cells have also been performed.

Grant support provided to D.K. and R.F. from the National Science Foundation and R.B. from the U.S. Department of Agriculture.

M-AM-F4 SULFIDE:CYTOCHROME c OXIDOREDUCTASE ACTIVITY OF CHROMATIUM VINOSUM FLAVOCYTOCHROME c_{552}.
D. Knaff[a], M. Davidson[a], F. Millett[b] and H. Bosshard[c]. [a]Dept. of Chemistry, Texas Tech Univ.; [b]Dept. of Chemistry, Univ. of Arkansas; [c]Biochemistry Inst., Univ. of Zürich.

C. vinosum flavocytochrome c_{552} consists of a 46 kD, FAD-containing and a 21 kD, heme c-containing subunit. The flavocytochrome transfers electrons from sulfide to cytochrome c_{550} and a number of related high potential cytochromes c, including equine cytochrome c. The K_m for equine cytochrome c increases with increasing ionic strength. V_{max} is unaffected. Evidence for complex formation between C. vinosum flavocytochrome c_{552} and its electron acceptors has been obtained by demonstrating that mitochondrial cytochromes c and C. vinosum cytochrome c_{550} bind to a flavocytochrome c_{552} affinity column. Also, flavocytochrome c_{552} binds to an equine cytochrome c affinity column. Increasing ionic strength, over the range that inhibits sulfide oxidation, elutes the cytochromes from the respective affinity columns. The heme-containing, but not the flavin-containing subunit of C. vinosum flavocytochrome c_{552}, binds to an equine cytochrome c affinity column, suggesting that the heme subunit contains the binding site for cytochrome c. ($CF_3PhNHCO$)-derivitization of five lysine residues surrounding the exposed heme edge of cytochrome c significantly increased the K_m for sulfide oxidation while modification of a distant lysine had no effect on K_m, implicating the five "front side" lysines in complex formation. Complex formation between C. vinosum flavocytochrome c_{552} and cytochrome c protects 4 front side lysines on cytochrome c from acetylation without shielding "back side" lysines, providing additional evidence for the role of specific front side lysines in complex formation.

Supported by grants from the Welch Foundation (to D.K.) and the N.I.H. (to F.M.).

M-AM-F5 THE ORIGIN OF THE PHOTOACOUSTIC EFFECT IN LEAVES FROM *IMPATIENS PETERSIANA*.
R. M. Leblanc, B. LaRue and A. Désormeaux, Centre de recherche en photobiophysique, Université du Québec à Trois-Rivières, C.P. 500, Trois-Rivières, Québec, Canada G9A 5H7.

The photoacoustic signal from intact leaves is the vector sum of two components which differ by their phases: one is the usual thermal contribution, the other originates from the periodic pressure increase related to modulated oxygen evolution. Since the two components respond differently to variables such as wavelength, chopping frequency or light intensity, time has come for a reappraisal of previously published data. Globally, the photoacoustic signal from the leaf consists of (i) An internal component which subdivides further into heat ($\vec{T}_1$) and oxygen ($\vec{O}$) production. This weak component is released rapidly; (ii) A photothermal surface component ($\vec{T}_2$), strong at its source (the chloroplast), but attenuated considerably before it reaches the leaf surface later on. This model is supported by the profile of the acoustic wave which results from a short, but intense light pulse followed by a much longer dark recovery period. Under these conditions where only the contribution of the photothermal component is significant, the initial acoustic burst is followed about 4 milliseconds later by a second wave. Because of differences in the diffusion lengths involved, the latter should correspond to the surface component. As a counterproof, water infiltration, which floods the intercellular air space, leads to a single wave profile for the same leaf sample. The present report of *Impatiens petersiana*, a common house plant, clarifies the structural origin of the photothermal component and shows how the morphology of the leaf distorts the spectroscopic information.

M-AM-F6 EVIDENCE FOR A MANGANESE TETRAMER IN THE O_2-EVOLVING COMPLEX OF PHOTOSYSTEM II.
Gary W. Brudvig, Julio C. de Paula, and Warren F. Beck, Department of Chemistry, Yale University, New Haven, CT 06511.

A number of EPR signals have been observed from the S_2 state of the O_2-evolving complex (OEC). These include: (i) three distinct multiline EPR signals with different magnetic properties (de Paula and Brudvig (1985) J. Am. Chem. Soc. 107, 2643) and (ii) a g=4.1 EPR signal (Casey and Sauer (1984) 767, 21). We find that the addition of ammonia produces another distinct S_2 state multiline EPR signal with altered hyperfine couplings and magnetic properties. This effect is specific for ammonia; other amines do not alter the S_2 state EPR signals. The temperature dependence of all five of these S_2 state EPR signals has been measured. These data can be accounted for by a model for the S_2 state of the OEC consisting of a 3Mn(III)-Mn(IV) tetramer in which two antiferromagnetically coupled Mn dimers are ferromagnetically coupled. The differences between the S_2 state EPR signals can be explained by varying the magnitude of the exchange couplings.

M-AM-F7 ^{35}Cl NMR STUDIES OF Cl^- ACTIVATION AND F^- INHIBITION OF PS-II. C.Preston and R.J. Pace, Botany Dept, and Research School of Chemistry, Australian National University, Canberra ACT Australia 2601.

Chloride ion activates oxygen evolution activity in PS-II with an apparent $K_{1/2}$ in the range of a few millmolar. We have used ^{35}Cl NMR T_2 relaxation enhancement to examine Cl^- interaction with PS-II in thylacoids and particles derived from mangrove (avicinia marina). Studies have been made on material in both the dark adapted (S_1) state and on other S states generated by flashing dilute PS-II suspensions within the spectrometer. These show that there is no NMR visible high affinity ($K_{1/2}$<0.5M) Cl^- binding in the dark state, but that high affinity Cl^- sites ($K_{1/2}$<10mM) are induced in the S_1 state by treatment with F^-, a potent inhibitor of oxygen evolving activity. Moreover, this F^- inhibition is totally non competitive with respect to Cl^-, suggesting separate sites of action for the two halide ions. The flash studies show that both the S_0 and S_1 states exhibit no high affinity Cl^- binding but that the S_2 and S_3 states display high affinity Cl^- binding similar to that induced by F^- in the S_1 state, and which activates oxygen evolution. These observations suggest a model in which the active site in the PS-II mangano protein (s) exists in two principal conformational states, one (S_0,S_1) which binds water (or hydroxide) but not Cl^- and one (S_2,S_3) which binds Cl^- and traps reaction intermediates (peroxide?). Bound F^- may force the system into the chloride binding S_2,S_3 conformational state by mimicking peroxide, presumably as a ligand to one or more of the Mn ions.

M-AM-F8 MEASUREMENT OF PLASTOQUINONE PHOTOREDUCTION IN SPINACH CHLOROPLASTS

S. W. McCauley* and A. Melis+
*Physics Dept. California State Polytechnic University, Pomona, CA 91768
+Mol. Plant. Biol. University of California, Berkeley, CA 94720

Measurements of photoreducible plastoquinone (PQ) concentration and its stoichiometry to photosystem I (PSI) and PSII in spinach chloroplasts will be presented. The results from three different experimental approaches are compared. (a) Quantitation from the light-induced absorbance change at 263 nm (ΔA_{263}) yields the following ratios (mol:mol); Chl:PQ = 70:1, PQ:PSI = 9:1 and $PQ:PSII_\alpha$ = 7:1. The kinetics of PQ photoreduction are a monophasic but non-exponential function of time. The deviation of the semi-logarithmic plots from linearity reflects the cooperativity of several electron transport chains at the PQ pool level. (b) Estimates from the area over the fluorescence induction curve (A_{f1}) tend to exaggerate the PQ pool size because of electron transfer via PSI to molecular oxygen (Mehler reaction) resulting in the apparent increase of the pool of electron acceptors. The reliability of the A_{f1} method is increased substantially upon plactocyanin inhibition by KCN. (c) Quantitation of the number of electrons removed from PQH_2 by PSI, either under far-red excitation or after the addition of DCMU to pre-illuminated chloroplasts, is complicated due to the competitive loss of electrons from PQH_2 to molecular oxygen. The latter is a biphasic reaction occurring with half-times of about 2 s (30-40°/o of PQH_2) and of about 60 s (60-70°/o of PQH_2). Possible reasons for the biphasic reaction will be discussed.

M-AM-F9 DETERMINATION OF DISSOLVED OXYGEN IN PHOTOSYNTHETIC SYSTEMS--A NITROXIDE SPIN PROBE BROADENING METHOD, by Shimshon Belkin, Rolf J. Mehlhorn, and Lester Packer

Concentrations of dissolved oxygen were monitored by following the width of the midfield line of the electron spin resonance spectrum of a nitroxide spin-probe. Measurements of peak-to-trough widths of first derivative spectra yielded accurate data over a high range of O_2 concentrations (up to 5 mM). Continuous traces of second harmonic line heights yielded similar results and proved to be advantageous for kinetic measurements, but were less sensitive at O_2 levels above 2 mM. Photosynthetic oxygen evolution and respiratory oxygen uptake in the cyanobacterium Agmenellum quadruplicatum were thus examined over a broad range of oxygen concentrations. Upon prolonged (>1 min) illumination, effects of photooxidative damage to both photosynthesis and respiration were demonstrated in the same experimental system. With the addition of an impermeable paramagnetic broadening agent, rapid transients in intracellular concentrations of dissolved O_2 could be measured.

M-AM-G1 CONTROL OF SPECIFICITY IN BIOLOGICAL ELECTRON TRANSFER, M.A. Cusanovich, T.E. Meyer, and G. Tollin, Department of Biochemistry, University of Arizona, Tucson, AZ 85721

Laser flash photolysis has been used to study the kinetics of electron transfer reactions to obtain an understanding of the factors controlling biological specificity. We have studied a variety of cytochromes c, cytochromes c', HiPIP's and copper proteins. Using eighteen homologous c-type cytochromes and lumiflavin semiquinone, we have shown a relationship between rate constants and the difference in redox potentials between reactants. This has allowed quantitation of steric effects for bulkier reactants, and using the negatively charged FMN semiquinone as the reductant, electrostatic effects on rate constants were also quantitated. Utilizing flavodoxin semiquinone as a reductant, the effects with free flavins were dramatically magnified in extent, although qualitatively they are similar.

The cytochromes c generally show a positive charge at the site of interaction. Ionic strength effects on rate constants for HiPIP, copper proteins, and cytochrome c' indicate that these proteins have a more uniform charge distribution than the cytochromes c. The implication of this for the biological function of these proteins is that electrostatic interactions are not as important as in the cytochromes c, where active site charge is highly conserved. In fact, significant steric control has been demonstrated in some cases.

Based on our studies to date, we can, in general terms, understand the kinetic control of redox reactions in complex mixtures where a variety of reactions are possible on thermodynamic grounds, thus understand the factors controlling biological specificity. This research was supported by NIH grants GM21277 and AM15057.

M-AM-G2 **LIGAND-CONTROL OF THE AGGREGATION STATE OF CHROMATIUM VINOSUM CYTOCHROME C'.** M.L. Doyle, S.J. Gill & M.A. Cusanovich*, Department of Chemistry & Biochemistry, University of Colorado, Boulder, CO 80309 and *Department of Biochemistry, University of Arizona, Tuscon, AZ 85721.

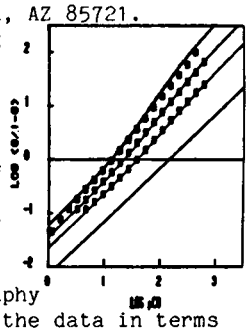

Cytochromes c' are isolated from a variety of photosynthetic and denitrifying bacteria. Their physical properties have been extensively studied but their biological role is unknown. The dimer R. molischianum cytochrome c', for which x-ray structural information is available, binds CO non-cooperatively (Doyle, M.L., Weber, P.C. & Gill, S.J. Biochemistry (1985) 24, 1987.). However, CO binding to the related dimer C. vinosum cytochrome c' is quite different. First, the adjacent Hill plot shows, for three protein concentrations (left-right ; 20, 70 & 250 μM heme), that the CO binding curve is cooperative (slope=1.2) and depends on protein concentration. Second, temperature-dependence studies and direct calorimetry give a large endothermic heat of CO binding (10 kcal/mol heme). These observations suggest ligand-linked changes in aggregation state. Gel chromatography shows the unligated form as a dimer and the ligated form as monomer. Evaluating the data in terms of a CO-linked aggregation process yields an aggregation constant for the ligated species as 450 ± 200 M^{-1} and a CO binding constant to the dimer as 5,600 ± 1,200 M^{-1} at 25°C. The heats of these reactions are determined as -38 ± 10 and -9 ± 5 kcal/mol respectively. From the observed free energy change of dissociation of the fully-ligated dimer (3.6 kcal/mol dimer) one finds a large entropy increase of 130 cal/deg-mol dimer which suggests a significant structural change in the subunits upon binding CO. (Supported by NIH grants HL 22325 (S.J.G.) & GM 21277 (M.A.C.).)

M-AM-G3 ELECTRON SELF-EXCHANGE IN CYTOCHROMES C. Dabney White Dixon and Michael Barbush, Department of Chemistry, Washington University, St. Louis, Missouri, 63130; Francis Millett, Department of Chemistry, University of Arkansas, Fayetteville, Arkansas 72701 and Russell Timkovich, Department of Chemistry, University of Alabama, University, Alabama 35486.

Electron self-exhange rate constants have been measured for a number of cytochromes using NMR line broadening methods. Eukaryotic cytochromes c measured to date are in the slow exchange limit; rate constants can be calculated from either the Fe(II) or Fe(III) resonances. The rate constants are in the range 1-2 x 10^4 M^{-1} s^{-1}. Electron self-exchange in fully trifluoroacetylated horse heart cytochrome c (19 lysine-$COCF_3$ groups) has been probed by both ^1H and ^{19}F NMR. The rate constant of this derivatized protein is approximately 10^5 M^{-1} s^{-1}. The activation energy for electron self-exchange of pigeon cytochrome c is 9 kcal mol^{-1} at 0.1 M ionic strength. Cytochrome c_{551} from Ps. aeruginosa has an electron self-exchange rate constant in the intermediate to fast exchange region (200 MHz and 1 mM). The rate constant is 1.3 x 10^7 M^{-1} s^{-1} in 0.05 M phosphate and 2.0 x 10^7 M^{-1} s^{-1} in 0.05 M phosphate with 0.5 M KCl. The mechanistic implications of these observations will be discussed. The work was supported by NIH grant AM 30479 to DWD.

M-AM-G4 RESONANCE RAMAN SCATTERING FROM HORSERADISH PEROXIDASE COMPOUND I, W. A. Oertling and G.T. Babcock, Dept. of Chemistry, Michigan State University, E. Lansing, MI 48824-1322.

Horseradish peroxidase (HRP) catalyzes the oxidation of various substrates in the presence of hydrogen peroxide by forming sequential intermediates, compounds I and II (HRP-I and HRP-II), which are two and one oxidation equivalents above the ferric state. Though resonance Raman (RR) techniques have been applied to the ferrous and ferric enzyme and to HRP-II, Raman data for HRP-I have been difficult to obtain owing to the reactivity and photolability of the first intermediate. Cryogenic techniques may be insufficient to stabilize HRP-I to laser irradiation and past attempts to obtain RR measurements of HRP-I resulted in photoreduction.[1] We have avoided these problems by using pulsed, near UV laser excitation of a flowing sample of HRP-I, which was generated by rapid mixing of native HRP with hydrogen peroxide. The flow rate insured that each laser pulse was incident on a fresh aliquot of sample.

Past RR spectra of HRP-II have been indicative of a 6-coordinate, ferryl low spin state. Contrasting the result obtained here for HRP-I with those obtained by other investigators for HRP-II reveals frequency decreases in normal modes possessing high percentages of both $\nu(C_\alpha\text{-}N)$ and $\nu(C_\alpha\text{-}C_m)$ character. These frequency shifts are interpreted in terms of loss of electron density from the π-bonding orbitals of the porphyrin ring upon oxidation as well as possible structural differences between the two species.[2]

This work was supported by NIH GM25480.

References: 1) Van Wart, H.E.; Zimmer, J. J. Am. Chem. Soc. 1985, 107, 3379-3381.
2) Oertling, W.A.; Babcock, G.T. J. Am. Chem. Soc., in press.

M-AM-G5 DYNAMICS OF HEME ACTIVE SITES AS MONITORED BY RESONANCE RAMAN Fe(IV)=O VIBRATIONS OF INTERMEDIATES OF HEME ENZYMES. Andrew J. Sitter, Catherine M. Reczek, and James Terner, Dept. of Chemistry, Virginia Commonwealth University, Richmond, VA 23284

Our laboratory has recently located Fe(IV)=O stretching vibrations of horseradish peroxidase compound II, ferryl myoglobin, and a number of other heme enzymes. We have found that the vibrational frequency of the Fe(IV)=O group is extremely sensitive to changes in the environment of the heme pocket. In horseradish peroxidase compound II, the Fe(IV)=O frequency will switch between two values as a function of pH. We have proposed that this behavior can be accounted for by the ionization of an amino acid group distal to the heme, probably a histidine, that is hydrogen bonded to the Fe(IV)=O group. The non-ionized hydrogen bonded form at neutral pH is the enzymatically active form. The ionized non-hydrogen bonded form at alkaline pH has greatly diminished activity. Horseradish peroxidase compound X is the initial product of the reaction of horseradish peroxidase with chlorite. Compound X has been proposed to contain a heme with an Fe(IV)-OCl group. Using isotopically labelled chlorite we have found that compound X actually contains an Fe(IV)=O group. Additionally, the Fe(IV)=O frequency of compound X displays a frequency shift as a function of pH, which is remarkably similar to that displayed by compound II. Our data suggests that compound X has the same heme stucture as compound II.

Support for this work is acknowledged from the Jeffress Memorial Trust, the National Institutes of Health (Grant No. BBCA 1R01 GM34443-01A1), and from an Alfred P. Sloan Fellowship (1985 to 1987) to J. Terner.

M-AM-G6 THE pi-CATION RADICAL OF Zn-CYTOCHROME c PEROXIDASE AND ITS INTERACTION WITH FERROCYTOCHROME c. H. Anni and T. Yonetani, Biochem./Biophys., Univ. Pennsylvania, Philadelphia, PA 19104.

Zn-protoporphyrin-substituted cytochrome c peroxidase (Zn-CCP) is aerobically converted upon illumination to a mixture of a reversible porphyrin pi-cation radical and irreversible porphyrin-oxidation products, both of which exhibit a low-intensity Soret band. The pi-cation radical is characterized by a 688-nm band, whereas the porphyrin oxidation products have absorption band at 498 nm. Several spin-trapping agents tested are found to be effective in increasing the yield of the pi-cation radical. pi-Cation radicals of Zn-CCP and Zn-horseradish peroxidase are compared for their ability to oxidize ferrocytochrome c in order to study the mechanism of electron transfer between cytochrome c peroxidase and ferrocytochrome c. Supported in part by research grants NSF PCM83-16935 and NIH HL14508.

M-AM-G7 VARIATIONAL THEORY FOR g-TENSOR USING ENERGY LEVELS AND WAVE-FUNCTIONS FROM LCAO-MO INVESTIGATIONS-APPLICATION TO FERRICYTOCHROME C AND AZIDOMYOBLOGIN, J.N. Roy[1], Santosh K. Mishra[1], K.C. Mishra[2] and T.P. Das[1]. (1) Department of Physics, State University of New York at Albany, New York, 12222; (2) GTE Sylvania Lighting Center, Danvers, MA, 01923. In recent work[1], we have studied the g-tensors in a number of heme compounds using a perturbation theory approach based on electronic energy levels and wave-functions from LCAO-MO investigations by the Self-Consistent Charge Extended Huckel Procedure. These investigations provided reasonable agreement between theory[1] and experiment[2,3]. However, for some systems, such as ferricytochrome c, the spin-orbit interaction was of comparable order as the separation between a pair of the d-like energy levels, requiring[1] the use of higher order perturbation theory. To remedy this problem and improve the accuracy of theory, we have, in the present work, carried out a variational approach involving the spin-orbit interaction and the Zeeman interaction of the magnetic moment of the electron with the applied magnetic field. Application has been made to ferricytochrome c and azidomyoglobin. The principal components of the g-tensor for the former are found to be (2.922, 1.995, 1.24), comparing well with the experimental values[2] of (3.06, 2.25, 1.24). For azidomyoglobin, the theoretical and experimental[3] results are respectively (2.63, 2.11, 1.81) and (2.80, 2.22, 1.72). These results provide support for the correctness of the calculated electronic structures. Possible directions for further improvement between theoretical and experimental g-tensors will be discussed. (Supported by NIH grant HL-15196).

1. Mishra S.K. et. al., Bull. Am. Phys. Soc. 30, 384 (1985); Mishra K.C. et. al., 30, 385 (1985).
2. Mailer C. and Taylor C.P.S., Can. J. Biochem. 50, 1048 (1972).
3. Dickinson L.C. and Chien J.C.W., J. Biol. Chem. 252, 1327 (1977).

M-AM-G8 MOLECULAR ORBITAL ANALYSIS OF G-TENSORS IN FERRIC BISIMIDAZOLE SYSTEMS WITH DIFFERENT DEGREES OF PROTONATION. J. N. Roy[1], Santosh K. Mishra[1], K. C. Mishra[2] and T. P. Das[1], 1) Department of Physics, State University of New York at Albany, Albany, New York 12222; 2) GTE Sylvania Lighting Center, Danvers, MA 01923 The dependence of the g-tensor on the degrees of protonation of imidazoles in ferric bisimidazole systems has been a subject of interest for some time[1]. Recently[2], EPR measurements have been carried out on a series of systems with fully protonated and partially and totally deprotonated imidazoles. Using a variational treatment[3] of the g-tensors based on electronic structures determined by the Self-Consistent Charge Extended Hückel procedure, we have investigated the g-tensors for these three types of bisimidazoles to compare with experiment. Our analysis showed that one needed small distortions of the porphyrin base from tetragonal symmetry, represented by the difference ΔR between N_1-N_3 and N_2-N_4 distances to explain the observed g-tensors. The ΔR were obtained by matching theory and experiment for smallest principal components of the g-tensors. Our values of the principal components in fully protonated and partially and totally deprotonated systems were respectively (1.53, 2.05, 2.75), (1.74, 2.05, 2.60), (1.72, 2.05, 2.65) as compared to experimental values[2] of (1.53, 2.26, 2.91), (1.74, 2.28, 2.73), (1.72, 2.24, 2.78). The values of ΔR obtained for the three systems were 0.076, 0.114 and 0.110 Å respectively corresponding to rhombic energy splittings of 310, 459 and 443 cm^{-1}. The possible sources for these splittings will be discussed (supported by NIH grant, HL-15196); 1) See for instance, Peisach J., Blumberg W. and Adler A., Ann. NY Acad. Sci. 206, 310 (1973); 2) Quinn R., Nappa M., and Valentine J. S., J. Am. Chem. Soc. 104, 2588 (1982); 3) Roy, J. N. et al. See our other abstract in these proceedings.

M-AM-G9 CALCULATED ELECTRONIC SPECTRA OF MODEL FERRIC CYTOCHROME P450 COMPLEXES

Ahmad Waleh, Jack R. Collins and Gilda Loew, SRI International, Menlo Park, California 94025

Restricted open-shell ground state and electronic spectra of two closely related low-spin, ferric, 6-coordinate, model cytochrome P450 complexes, one with a methyl mercaptide and the other a mercaptan as the second axial ligands, have been calculated with a newly-modified, semi-empirical INDO-SCF-CI method. The sensitivity of the calculated spectra to protonation of the sixth axial ligand, and the ability of the method to predict characteristic spectral features for the complexes investigated are determined. Assignment of the transitions, including xy- and z-polarized transitions, are made and compared with experimental observations where available. In particular, the origin of the anomalous split Soret spectrum observed in low-spin ferric complexes with mercaptide but not a mercaptan is investigated. Finally, a two part hypothesis is presented which provides a general explanation for the origin of both the observed Soret and the red-shifted normal Soret in various ferrous and ferric P450 complexes in terms of the ground state orbital character and simple symmetry considerations.

M-AM-G10 TRANSITION INTERMEDIATES OF HEMOGLOBIN S CRYSTALIZATION

William A. McDade, Robert J. Vassar and Robert Josephs
The University of Chicago, Department of Molecular Genetics and Cell Biology

The pathological manifestations found in sickle cell anemia are due to the vaso-occlusive episodes that occur when mutant hemoglobin polymers distort and rigidify the red blood cell. Crystallizing deoxygenated hemoglobin S (HbS) forms a series of intermediate structures in stirred solutions. A pathway whose bifurcation is governed by a transition pH yields macrofibers under more acidic conditions while fascicles of fibers obtain under more alkaline conditions. There are common structural features shared between the particles of either pathway in that both are composed of double strands of polymer filaments and both yield structurally identical crystals. It is the mode in which the filaments pack that distinguish the classes. As a class, macrofibers show typical changes in helical pitch and the number of double strands they contain as they develop into crystals. The final transition to crystalline order from macrofibers involves direct fusion of formed particles. As crystallization proceeds, fascicles of fibers display a remarkable transition into bundles of particles registered in an ordered lattice. Based upon the analysis of helical pitch, cross sectional diameter and packing formation it appears that lateral alignment is a necessary condition for unwinding of helical progenitors of crystalline HbS. Through direct observation of samples prepared for electron microscopy and indirect seeding experiments with solutions of HbS intermediates, a continuous transition between these structures is indicated. This continuity implies minor rearrangements between associating particles while militating against complete dissolution and renucleation of later intermediate structures.

M-AM-G11 DIFFERENTIAL POLARIZATION IMAGING MICROSCOPY OF ALIGNED INTRACELLULAR HEMOGLOBIN S POLYMER: THE EFFECTS OF FIXATION AND SPEED OF DEOXYGENATION OF ALIGNED HEMOGLOBIN S.

Wm. Mickols, I. Tinoco, Jr., M. F. Maestre, S. E. Embury, University of California, Berkeley, Lawrence Berkeley Laboratory, University of California, San Francisco.

Linear dichroism imaging of sickled red blood cells (RBCs) indicates the amount of aligned hemoglobin (Hb) and its orientation as a function of position within the cell (Proc. Natl. Acad. Sci. USA 82, 6527-6531 (1985)). The usual intensity image provides the distribution of total Hb within the cell. From these two images we can compute an image of the ratio of aligned Hb to total Hb. These images clearly show a non-uniform distribution of the aligned Hb, and the separation of some aligned polymer from total Hb within the cell.

Cells with obvious multiple nucleation sites have been seen. This lends experimental support to recent proposals of multiple nucleation as an important in-vivo sickling route.

Two rates of deoxygenation were studied to compare rate with amount of aligned intracellular Hb. Slowly deoxygenated samples (linear decrease in O_2 over 1 hr.) showed an increase by about a factor of two in aligned Hb vs. quickly deoxygenated samples (direct injection into deoxygenated buffer).

Comparison of fixed and unfixed RBCs indicate that about half the measured linear dichroism is lost during fixing. There is a large cell to cell variation in linear dichroism in all samples.

M-AM-G12 **STUDIES OF DEOXY SICKLE CELL HEMOGLOBIN AGGREGATES UNDER NON-GELLING CONDITIONS BY SPIN LABEL EPR TECHNIQUES.**

Chung Jeing Yuan, Chao Chuan Hu and Michael E. Johnson. Department of Medicinal Chemistry, University of Illinois at Chicago, Chicago, Illinois 60680.

Tempo-maleimido spin labeled deoxy sickle hemoglobin (HbS) and deoxy normal adult hemoglobin (HbA) have been examined by conventional and saturation transfer electron paramagnetic resonace (EPR) techniques. The measured spectral parameters, i.e., the hyperfine separation from the conventional spectrum and the L''/L ratio from the saturation trasfer spectrum, can be respectively converted into effective correlation times. The calculated correlation times of deoxy HbS are consistently slightly longer than those of deoxy HbA at various concentrations and temperatures, although no gel polymer is observed in any of the samples. This indicates that deoxy HbS exhibits a limited aggregation under non-gelling conditions. We have proposed a thermodynamic model that successfully accounts for the observed correlation times of deoxy HbS with respect to its total concentration in comparison with the correlation times of the monomeric deoxy HbA molecule. Analysis of this apparent aggregation also indicates that it is independent of temperature. The significance of these results will be discussed in relation to previous work suggesting the existence of HbS aggregates under non-gelling conditions.

(Supported in part by grants from the US National Institutes of Health.)

M-AM-H1 EFFECT OF SOME DIVALENT CATIONS ON pH REGULATION IN BALANUS PHOTORECEPTOR. H. Mack Brown and Daniel Erne.

Intracellular Cl^- and extracellular Na^+ have been found to be necessary for maintenance of intracellular pH (pH_i) in a number of preparations. There have been few reports that extracellular divalent cations affect these pH regulating mechanisms. We have found evidence for a HCO_3^-/Cl^- exchange mechanism in Balanus photoreceptors and have examined the influence of Ca^{2+} and Co^{2+} on regulation of intracellular pH. We find that (1) external Ca^{2+} is necessary for maintenance of pH_i and (2) that extracellular Co^{2+} blocks recovery of cellular acidification. Intracellular pH_i was assessed with microelectrodes containing the liquid membrane tri-n-dodecylamine. The cells were acidified with either CO_2 or by illuminating them. Preliminary experiments indicate that an Na^+/H^+ acid extrusion mechanism is not operational in this photo-receptor since pH recovery from acid loads (CO_2) appears normal in Na^+-free saline. On the other hand, a Cl^-/HCO_3^- system is suggested by the observations that extracellular HCO_3^- is necessary for pH recovery from an acid load and washout of intracellular Cl^- in Cl^--free medium produces cellular alkalinization and retards pH recovery from an acid load. Removal of Ca^{2+} (+1 mM EGTA) from the medium also alkalanizes the cell (0.2 pH), but does not appear to block pH recovery from a light flash. Addition of Co^{2+} to the medium has much different effects: (1) pH_i acidifies in the dark, (2) the effects of acidification by light is augmented by as much as 200% and (3) pH recovery from an acid load is considerably retarded. These results indicate that external Ca^{2+} plays a role in pH maintenance in this photoreceptor but is not necessary for pH changes induced by light. Other divalent cations can have profound inhibitory effects on pH regulation. (NIH EY 00762)

M-AM-H2 INJECTION OF PHOSPHOLIPASE C INTO LIMULUS VENTRAL PHOTORECEPTORS. L. J. Rubin, J. E. Brown and M. Poznansky*. Dept. Ophthalmol., Wash. Univ. Sch. Med., St. Louis, MO. and *Dept. Physiol., Univ. Alberta, Edmonton, Canada.

After intracellular injection of phospholipase C solutions into Limulus ventral photoreceptors: (1) the membrane potential became more positive (often to zero or more positive than zero volts); (2) the cells' responsiveness to light decreased, and (3) the response to a bright light often became negative-going. Replacing 90% of the NaCl with sucrose partially repolarized the membrane of an injected cell, but the response to bright light continued to be negative-going. After phospholipase C was injected into a cell voltage-clamped to normal dark, resting potential, there was: (1) an increase in dark inward current; (2) a decrease in light-induced current, and (3) an outward current often was induced by bright light. These effects occurred even when Ca^{++} was omitted from the sea water. All these effects were induced by injection of phospholipase C from Bacillus cereus (Sigma; Calbiochem.) and by a purified phosphatidylinositol-specific phospholipase C (B.cereus) but not by phospholipase C from Clostridium perfringens (Sigma) or Staphalococcus aureus (Dr. M. G. Low). Phospholipase A_2 (Sigma: porcine pancreas or Vipera russelli) or phospholipase D (Calbiochem:peanut) were also without effect. Intracellular injection of boiled phospholipase C (B. cereus) or addition of phospholipase C (B. cereus) to the sea water bathing a denuded photoreceptor cell did not have an effect even at enzyme activities exceeding those within injected cells. However, perfusing the same denuded photoreceptor cell with a sea water solution containing phospholipase A_2 (bee venom) rapidly disrupted the cell membrane. (Supported by EY 05166 and EY 05168)

M-AM-H3 RAPID FORMATION OF INOSITOL TRISPHOSPHATE ($InsP_3$) IN SQUID PHOTORECEPTORS. S.F. Wood+, M.S. Reid, E.Z. Szuts, and A. Fein. Boston University Marine Program+ and Laboratory of Sensory Physiology, Marine Biological Laboratory, Woods Hole MA 02543.

$InsP_3$ appears to be a second messenger for calcium mobilization, and mimics light when injected into Limulus ventral photoreceptors. To determine whether light regulates $InsP_3$ in invertebrate photoreceptors, $InsP_3$ levels were measured in squid eyes, whose large number of photoreceptors ($\sim 10^7$) occupy most of the retinal volume. Four half-eyecups from the same animal were incubated for three hours at 10 °C in oxygenated artificial sea water with ^3H-inositol. The eyecups remained light-sensitive after incubation, as measured by electroretinograms. Two half-eyecups were flashed with intense light (~1ms duration) and their reactions quenched by immersion into liq. Freon 22(<-100 °C) at various times after the flash. The remaining half-eyecups served as dark controls. By measuring the temperature behind the eyecup with fine thermocouples, the freezing time of the receptor-distal segments (300μm in length) was calculated to be 0.15±0.08s after immersion. Extracted inositol phosphates were separated by ion exchange chromatography. Following a flash, $InsP_3$ increased 3-4 fold over dark controls and remained elevated for up to 2min. The light/dark ratios (L/D) for $InsP_3$ at various intervals between flash and immersion are shown on right as mean±s.d. (no. of exp.). Dark controls varied less than 15%. $InsP_2$ did not vary in response to light: L/D=1.03±0.22 (n=21) at 3.0s. Our results suggest that light-stimulated formation of $InsP_3$ is rapid enough for its involvement in adaptation and possibly excitation of squid photoreceptors.

-1.0s	1.20±0.48	(6)
0.125s	3.60±1.23	(6)
0.5s	2.36±1.07	(4)
3.0s	3.36±1.60	(26)
10.0s	5.33±1.58	(4)
2.0min	2.26±1.09	(5)

M-AM-H4 PRESSURE INJECTION OF CALCIUM INTO LIMULUS PHOTORECEPTORS ACTIVATES THE LIGHT-SENSITIVE SODIUM CONDUCTANCE. Richard Payne, D. Wesley Corson, Alan Fein, Marine Biological Laboratory, Woods Hole, MA 02543.

Brief (<500ms) pulsed pressure-injection of 1-10 pl of 2 mM calcium aspartate or $CaCl_2$ into the light-sensitive region of Limulus ventral photoreceptors results in a 20-40 mV depolarization, lasting approximately 2s. The depolarization closely follows the rise in intracellular free calcium, as indicated by aequorin luminescence. Subsequent responses to light are reversibly diminished. Similar injections into the light-insensitive region of the receptor are essentially without effect, although aequorin luminescence indicates a rise in free calcuim. Prior injection of calcium buffer abolishes all of the effects of calcium injection. Injection of 2 mM Sr also depolarizes and desensitizes the photoreceptor. 2mM Ba does not depolarize the photoreceptor, but it desensitizes subsequent responses to light. Injection of 2mM Mg has no effect.

The depolarization caused by calcium arises from an inward current, amplitude 10-20 nA, having a reversal potential (+10 to +20mV) and rectification similar to those of the light-activated conductance. The reversal potentials of the light- and calcium-activated currents decrease similarly by 23-35 mV when 3/4 of the extracellular Na is replaced by sucrose, but are unaffected by a similar replacement of Na by Li. We suggest that calcium activates the light-sensitive channels. This may explain the ability of inositol-1,4,5-trisphosphate to activate the light-sensitive conductance via the release of calcium from internal stores.

M-AM-H5 INOSITOL TRISPHOSPHATE STIMULATES Ca^{2+} RELEASE FROM TOAD RETINAL ROD OUTER SEGMENT PREPARATIONS. Kenton R. Parker, Jonathan A. Briggs, Edward A. Dratz, Chemistry Department, University of California, Santa Cruz, CA 95064.

Inositol trisphosphate has been shown to induce the release of calcium from intracellular storage sites in many different tissues (Berridge and Irvine, 1984, Nature), including Limulus photoreceptors (Brown, et al., 1984, Nature; Fein, et al., 1984, Nature). In vertebrate photoreceptors light-induced hydrolysis of phosphatidylinositol 4,5-bisphosphate (PIP_2), has been reported (Ghalayini and Anderson, 1984, BBRC) and injection of IP_3 into salamander rods induces a reversible hyperpolarization of the rod membrane (Waloga and Anderson, 1985, BBRC). We have investigated effects of IP_3 on calcium activities in toad (Bufo marinus) rod outer segment preparations with permeabilized plasma membranes using Ca^{2+} selective mini-electrodes. In 12 out of 15 experiments we have observed large IP_3 dependent Ca^{2+} releases; a range of 0.8-5.4 x 10^5 Ca^{2+} ions are released per disk with addition of 5-10 μM IP_3. We obtain a similar range of Ca^{2+} efflux with the addition of 120-250 μM GMP. The maximum rate of Ca^{2+} efflux observed is approximately 3 x 10^4 Ca^{2+} ions $sec^{-1}disk^{-1}$. Addition of IP_3 to the system prior to cGMP attenuates the cGMP signal in most cases. In experiments where no ATP was added to the system during the preparation, the IP_3 induced signals were much smaller than previously observed with ATP. Upon addition of ATP, Ca^{2+} uptake is observed and the subsequent IP_3 signal was increased in size. Final medium includes NaCl, 10mM; KCl, 110mM; KH_2PO_4, 2mM; $MgCl_2$, 2mM; HEPES, 20mM; pH 7.4; ATP & GTP, 3mM; Creatine PO_4, 20mM and CPK, 16 U/ml. Toads were dark adapted 24-48 hours and all work was performed under infrared illumination. Supported by NIH EY00175.

M-AM-H6 COMPUTER SIMULATION OF THE LIGHT RESPONSE OF VERTEBRATE RODS. David C. Torney and Mark W. Bitensky. (Intr. by George Bell) Los Alamos National Laboratory, Los Alamos NM 87545

The hypothesis that the free pool of cyclic GMP is the principal regulator of the plasma membrane cation channel in the rod outer segment is investigated by computer simulation of the following sequence of reactions. (1) In the disk membrane bleached rhodopsin catalyzes conversion of G-protein upon encounter releasing Gα-GTP which then diffuses freely in the cytoplasm. (2) Gα-GTP reversibly binds to PDE (Phosphodiesterase) causing PDE activation. (3) Active PDE converts cyclic GMP to GMP at the disk-cytoplasm interface. (4) Cyclic GMP in the cytoplasm reversibly binds to the cation channels in the plasma membrane. The simulation addresses the points of specific regulation and the kinetic constraints of the light-sensitive "cascade" and makes contact with experimental measurements of membrane conductance in rod outer segments and isolated plasma membrane patches.

M-AM-H7 THE IMPORTANCE OF SCHIFF BASE DEPROTONATION IN THE FORMATION OF ACTIVATED RHODOPSIN. Colin Longstaff, Roger D. Calhoon, and Robert R. Rando, Department of Pharmacology, Harvard Medical School, Boston, MA 02115.

Metarhodopsin II is the spectroscopically defined conformer (or conformers) of photolyzed rhodopsin which apparently catalyzes the exchange of GTP for GDP bound to the G protein resulting in the activation of the latter. This is the only known biochemical event directly influenced by rhodopsin. Metarhodopsin II is generated from its precursor Metarhodopsin I with the concomitant uptake of protons. At the same time, however, the protonated Schiff base of Metarhodopsin I is deprotonated at Metarhodopsin II. We wish to answer whether this deprotonation is obligate in the formation of activated rhodopsin. We have approached this question by asking whether rhodopsin containing a methyl group adducted to its active-site lysine can achieve a Metarhodopsin II-like state after photolysis and activate the G protein.

Rhodopsin was reductively methylated leading to the incorporation of approximately 20 methyl groups (there are 10 non-active-site lysines). Upon photolysis, this pigment activates the G protein 107 ± 5% as well as unmodified rhodopsin. The bleached pigment was further methylated and then regenerated to yield active-site lysine monomethylated rhodopsin. This modification procedure produced a stable pigment with a λ_{max} = 520 nm. Bleaching of this material produced a long-lived Metarhodopsin I-like product (λ_{max} approx. 480 nm) which decayed over a period of hours at 4°C to all-trans-retinal and opsin. The bleaching of this pigment did not lead to the activation of G protein as revealed by its GTPase activity. These results are consistent with a mechanism in which there is an obligate loss of a proton from the Schiff base in the formation of the activated form of rhodopsin. Supported by N.I.H. grant EY-03624.

M-AM-H8 The role of ATP in cGMP-sensitive Ca^{2+} transport by ROS disks John S. George and Mark W. Bitensky, Life Sciences Division
Los Alamos National Laboratory, Los Alamos, NM 87545

We have studied Ca^{2+} metabolism in concentrated preparations of isolated, leaky rod outer segments (ROS). Miniature Ca^{2+} and pH electrodes were used to monitor ion activities. In other experiments, suspension aliquots were withdrawn and stabilized for nucleotide analysis by HPLC. We have identified two competing cGMP-regulated Ca^{2+} transport activities in ROS disks: ATP dependent Ca^{2+} uptake is stimulated by cGMP; cGMP hydrolysis can release significant quantities of previously loaded Ca^{2+}. Ca^{2+} uptake was the dominant process under experimental conditions where a high ATP/ADP ratio was produced by excess creatine phosphate (CrP). In such preparations, the addition of cGMP [$\geq$0.1mM] initially stimulated Ca^{2+} uptake even following total bleaching.

ROS ATPase activity appears to drive Ca^{2+} uptake indirectly, by generating a proton gradient across the disk membrane which in turn drives H^+/Ca^{2+} exchange. cGMP stimulates apparent ATPase activity. ATP hydrolysis by a model enzyme system containing Apyrase or by ROS preparations at pH $\geq$7.0 caused net acidification, however , at pH $\leq$6.0 ATP hydrolysis by ROS alkalinized the medium, possibly reflecting H^+ transport into disks. In ROS or model enzyme systems, ATP hydrolysis coupled to regeneration from CrP caused alkalinization. cGMP stimulated ATP dependent alkalinization by ROS in the presence of CrP, with a timecourse closely matching the stimulation of Ca^{2+} uptake. Stimulated alkalinization in response to cGMP was observed even when ROS Ca^{2+} uptake was inhibited by CCCP. ATP hydrolysis by ROS, measured by HPLC. was stimulated >2-fold by 0.5mM cGMP. < 1/3 of the additional hydrolysis of ATP could be attributed to regeneration of GMP produced by cGMP hydrolysis. (Supported by NIH grant AM31610)

M-AM-H9 SOME EFFECTS OF CYCLIC GMP ON PHOTO-TRANSDUCTION. Shaul Hestrin and Juan Korenbrot. Department of Physiology, U.C.S.F., San Francisco, CA 94143.

The effects of internal perfusion of cGMP were studied in rods of tiger salamander. We recorded photocurrent from isolated rods (w/o enzyme), using the "whole-cell" configuration of the patch-clamp technique. When cGMP was not added to the patch pipette the photoresponse was similar to the response of an intact cell.* Addition of 5mM cGMP to the pipette induced a large dark current (more negative than 500 pA) that could be supressed by light. This large dark current was not sustained for more than a few minutes in most of the cells. It is possible that the cells were overloaded with Na^+ and Ca^{++} which diminished the dark current. The response to flashes of light, during the initial period of the perfusion, was considerably prolonged and in most cells also had a longer delay and slower rate of rise. In the presence of dim background the dark current was reduced to low levels (~-100 pA). Under these conditions the recording lasted for longer periods of time. The amplitude of the dark current of light adapted cell could be increased by reducing the background illumination. The inital rise of the photocurrent in these light adapted cells, was similar to that observed in intact cells. However, the response to bright flashes of light was followed with a pronounced transient rebound that could be as large as -300 pA. The amplitude of the rebound was larger (more negative) when the flashes were brighter.

*as recorded by the suction pipette method.

M-AM-H10 EFFECT OF DIVALENT CATIONS ON THE MACROSCOPIC cGMP-ACTIVATED CURRENT IN EXCISED ROD MEMBRANE PATCHES. K.-W. Yau and L.W. Haynes, Univ. Texas Med. Branch, Galveston, Texas 77550.

The effect of divalent cations on the cGMP-activated current was studied in an excised, inside-out patch of toad rod outer segment membrane in visible light. The patch pipet contained normal Ringer's solution (with 1.6 mM $MgCl_2$ and 1.0 mM $CaCl_2$), while the bath contained a pseudo-intracellular low Na-high K solution with cGMP. Without bath divalent cations, the I-V relation for the cGMP-activated current showed very steep outward rectification. With 0.16 mM Mg^{++} in the bath, the current was reduced at depolarizations but was little affected at hyperpolarizations. The net result was a shallowing of the outward rectification; this shallowing increased progressively with Mg^{++} concentration. A similar, but less pronounced, effect was observed with Ca^{++} in place of Mg^{++} in the bath. The effects of Mg^{++} and Ca^{++} summated only to a degree; for example, in the presence of 1.6 mM Mg^{++} the addition or omission of Ca^{++} made little difference.

In other experiments where divalent cations were absent in both the pipet and the bath solutions, the recorded cGMP-activated current was generally much larger and the I-V relation became almost linear.

These results indicate that divalent cations have a suppressing effect on the cGMP-activated conductance (= the light-sensitive conductance). This suppressing effect, however, is unlikely to be involved in the generation of the light response because, as pointed out above, the conductance is little affected at hyperpolarizing potentials (where a rod is normally sitting) when normal Ringer's is present externally.

M-AM-H11 SINGLE cGMP-ACTIVATED CHANNELS RECORDED FROM EXCISED ROD MEMBRANE PATCHES. L.W. Haynes, A.R. Kay and K.-W. Yau (Intro. by R. Baker), Univ. Texas Med. Branch, Galveston, Texas.

Current was recorded from an excised, inside-out patch of toad rod outer segment membrane in visible light. Identical solutions (118 mM NaCl, 0.1 mM Na-EGTA, 0.1 mM Na-EDTA, and 5mM Na-HEPES, pH 7.6) were present in the patch pipet and the bath. With 1-5 μM cGMP in the bath, current fluctuations appeared at depolarizations and hyperpolarizations which resembled openings and closings of individual ion channels (see figure). At +60 mV, the prominent unitary current showed an amplitude of 1.3-1.7 pA and a roughly exponential distribution of open times (mean ∿ a millisecond). Both individual openings and short bursts of openings were observed. The unit current amplitude varied approximately linearly with voltage, corresponding to a conductance of ∿ 25 pS. The frequency of events increased with both cGMP concentration and depolarization. Upon adding 0.5 mM Mg^{++} to the bath solution the unitary current became largely unresolvable; the effect of Ca^{++} was similar but less pronounced. Besides events of the above size there appeared to be smaller events which might represent other states of the conductance.

Our results indicate that the cGMP-activated conductance (= the light-sensitive conductance) in rods is a channel rather than a carrier, and that in the absence of divalent cations it has a unit conductance similar to those of other channels. The suppression by divalent cations probably explains why single light-sensitive channels have not been resolved under normal conditions.

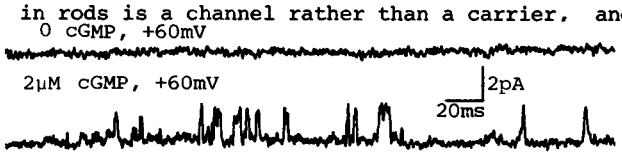

M-AM-H12 NOISE PROPERTIES OF cGMP-DEPENDENT CONDUCTANCE OF RETINAL RODS: EVIDENCE AGAINST A TWO-STATE CHANNEL MODEL. Gary Matthews, Dept. of Neurobiology, SUNY, Stony Brook, NY 11794

Cyclic GMP opens a cationic conductance when applied to the inner face of rod outer segment membrane patches. In a two-state model in which channel opening and closing are controlled by cGMP binding and unbinding, binomial statistics predict that as the mean level of current is increased by raising agonist concentration, the variance should initially increase, then decline as saturation is approached. Instead, however, variance was found to increase along with mean level up to saturation of the cGMP-dependent current. Power spectral analysis revealed that the variance increase could be attributed to a progressive rise in a high-frequency component of noise as concentration of cGMP was increased. At low concentrations (mean current <0.25 of saturation), the power spectral density could be approximated by the sum of a low-frequency, single-Lorentzian component with a corner frequency of 50-100 Hz and a high-frequency component that was flat to >2000 Hz. The Lorentzian component could not be readily resolved in all experiments. As cGMP concentration was increased, the high-frequency component was increasingly dominant, and at saturation the spectrum was approximately flat over the resolvable frequency range. These observations are consistent with models in which the open channel rapidly flickers, producing a high-frequency component of noise that increases with the number of open channels. An example of such a model is that the conducting state of the channel is governed by two gates, one that opens when cGMP is bound and another that flickers open and closed under the control of some other event. Firm test of this suggestion will require resolution of the cGMP-dependent conductance at the single-channel level. (Supported by NIH grant EY03821.)

M-AM-H13 EFFECTS OF BLEACHING AND BACKGROUND LIGHTS ON SENSITIVITY AND LIGHT-SUPPRESSIBLE CURRENT IN RODS OF AMBYSTOMA TIGRINUM. M. Carter Cornwall, Alan Fein, Paul Brown, Boston University School of Medicine, Boston MA 02118, Marine Biological Laboratory, Woods Hole, MA 02543 and Biological Laboratories, Harvard University, Cambridge, MA 02138.

Our previous work suggests mechanistic differences between bleaching and dim background adaptation in rods. We here report experiments which compare the spatial spread of background and bleaching adaptation as well as examine the relationship of sensitivity to light-suppressible current. Electrophysiological measurements using extracellular suction pipettes were performed on rods mechanically isolated from dark adapted tiger salamander retinas. Measurements of spatial spread of bleaching and background adaptation were compared by recording extracellular current from the inner segment while stimulating the outer segment with transverse focused slits of bleaching and dim background light. The space constant for spread of bleaching adaptation averaged less than 3 μm whereasthat for the spread of background desensitization averaged 6.9 μm. Local bleaching adaptation persisted for at least 2 hours whereas recovery following dim background light was complete within 1 minute. Recovery from bleaching adaptation (60% bleach) of both light-suppressible current and sensitivity was produced by exposure of the outer segment to a 2% ethanolic solution containing 20 μg/ml 11-cis retinal. In contrast, exposure of the outer segment to a solution containing 100uM IBMX resulted in recovery of the light-suppressible current to control levels during exposure to the drug with no change in sensitivity. These data suggest that important differences exist between biochemical steps which mediate bleaching and background adaptation, and that the desensitizing effects of bleaching adaptation are separable from those that control the magnitude of the light-suppressible current. Supported by HIH grants EY01157 and EY03793.

M-AM-H14 REGENERATIVE ELECTRICAL ACTIVITY IN THE ISOLATED CONE PHOTORECEPTOR: A VOLTAGE CLAMP ANALYSIS. A.V. Maricq* and J.I. Korenbrot, *Dept. of Biophysics, Univ. of Calif., Berkeley, CA 94720, and Dept. of Physiology, Univ. of Calif., San Francisco, CA 94143.

Isolated cone photoreceptors were enzymatically dissociated from the retina of the lizard, Sceloporus orcutti. The cone cells, usually remained morphologically intact although often they lacked their fragile outer segment.

Whole-cell clamp recordings were conducted in the light. Patch electrodes were filled with potassium aspartate, 4 mM ATP and buffered with HEPES and 10 mM EGTA. Under current clamp conditions the cells maintained a resting potential of approximately -30 to -35 mv and responded to hyperpolarizing current pulses with a distinctive decaying voltage peak, and a regenerative depolarizing voltage response upon termination of the current pulse. This latter response has a distinct spike, followed by a plateau phase of many hundred msec., and upon repolarization often oscillated at 2 to 3 Hz for many seconds between fast depolarizing spikes and repolarization (Fig. A - pulse duration = 2.5 sec.). This pattern of spike, plateau, and oscillating spikes was even more prevalent during depolarizing pulses.

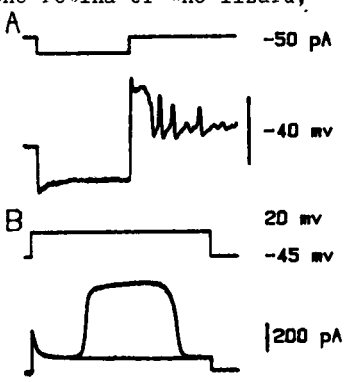

The voltage response to hyperpolarizing current was abolished by 5-10 mM CsCl added to the bath, and could be seen in voltage clamp to be the result of an inward current slowly activated by hyperpolarizations more negative than -45 mv and with a reversal potential of approximately -15 mv. The regenerative activity resulting from depolarizing the cell membrane is initiated by an inward calcium current, and shaped by a complex interaction between the calcium current and several outward currents. Specifically the decay of the plateau phase is modulated by a delayed calcium activated net outward current which can be blocked by 1 mM Cd++, 2-4 mM Mn++, or depolarizing prepulses (Fig. B pulse duration = 8.5 sec).

M-AM-I1 ALTERATION OF ENZYME FLEXIBILITY: MECHANISM OF INHIBITION OF Na^+,K^+-ATPase BY A MONOCLONAL ANTIBODY. William J. Ball, Department of Pharmacology and Cell Biophysics, University of Cincinnati College of Medicine, Cincinnati, OH 45267.

A monoclonal antibody (designated (MIO-P5-C11) has been prepared against the purified lamb kidney Na^+,K^+-ATPase. This antibody binds with high affinity to the catalytic subunit of the "native" holoenzyme and it inhibits greater than 90% of the enzyme's ATPase activity. Antibody M10-P5-C11 acts as a noncompetitive or mixed inhibitor with respect to the Na^+,K^+ and ATP dependence of the ATPase hydrolytic activity. It also inhibits the Na^+,Mg^{2+}-ATP-dependent phosphoenzyme intermediate formation, without effecting either the K^+-dependent p-nitophenylphosphatase activity, or dephosphorylation of the phosphoenzyme intermediate. Despite the inhibition of phosphoenzyme intermediate formation the antibody caused no decrease in ATP binding. Therefore the antibody prevents E~P intermediate formation without effecting either ATP binding or the dephosphorylation steps of the catalytic reaction. M10-P5-C11 binding appears to restrict the enzyme's conformational flexibility which allows the transfer of the γ-phosphate of ATP to the phosphorylation site after ATP binding at its binding site has occurred. These studies also demonstrate the existence of an enzyme-Mg^{2+}-ATP transitional intermediate preceding the formation of the ADP-sensitive E_1-P phosphoenzyme intermediate. (Supported by NIH Grant RO1-HL32214 and an Established Investigator Award from the American Heart Association.

M-AM-I2 INHIBITION OF THE Na,K-ATPase BY H_2DIDS. C.H. Pedemonte and J.H. Kaplan, Department of Physiology G4, University of Pennsylvania, Philadelphia, PA 19104

Treatment of partially purified Na,K-ATPase from canine renal medulla with 4,4'-diisothiocyano-1,2-diphenylethane-2,2'-disulfonic acid (H_2DIDS) results in inhibition of both Na,K-ATPase and K-phosphatase activities with a high apparent affinity (~3 uM). The presence of ATP or K in the incubation media with 60 uM H_2DIDS completely prevented inactivation with a high apparent affinity (50 uM for K and 12 uM for ATP), Mg produced only a partial protection with a low affinity. AMP and UTP were without effect; Na produced only a small protective effect with low affinity but counteracted the protective effect of K with a high affinity ($K_{0.5}$ - 1.5 mM). Analysis of the kinetics of the H_2DIDS-enzyme interaction showed reversible and irreversible (covalent) binding, both resulting in inhibition. None of the ligands, Na, K, Mg or ATP affected the reversible inhibition. 4,4'-dinitro-2,2'-stilbene disulfonic acid (DNDS) reversibly inhibited the Na,K-ATPase activity with low affinity (K_i=2.4 mM). DNDS also prevented the irreversible inhibition of the enzyme by H_2DIDS. The characteristics of the inhibition by H_2DIDS suggest that initially a reversible interaction occurs between the sulfonic acids and (presumably) positively charged side chains of the protein. This is followed by covalent reaction and attachment of the reduced stilbene via reaction of the isothiocyano group to a specific functional group (probably amino) on the protein. The covalent attachment occurs at a site which is ligand-protectable. Analysis of the binding of radiolabelled inhibitor suggests that only a small number of amino acid residues are involved in the inhibition. Supported by NIH HL 30315 and RCDA HL 01092.

M-AM-I3 CRYSTALLIZATION OF Na,K-ATPase BY LANTHANIDE IONS. H. C. Beall[1], D. F. Hastings[2], L. Dux[3], H. P. Ting-Beall[1] and A. N. Martonosi[3]. Depts. of Anatomy[1] and Physiology[2], Duke Univ. Med. Ctr., Durham, NC 27710, and [3]Dept. of Biochemistry, SUNY Upstate Med. Ctr., Syracuse, NY 13210.

It has been proposed that the active transport of Na^+ and K^+ involves two transitional conformations ($E_1 \rightleftarrows E_2$) of the ATPase. Results from other laboratories on tryptic proteolysis and intrinsic fluorescent intensity differences in the presence of Na^+ and K^+, suggest that the transition between E_1 and E_2 forms of the enzyme involves rearrangement of a large number of amino acid residues in the polypeptide chains. These structural changes are associated with occupancy of Na^+ binding sites on the cytoplasmic surface in E_1 state, or occupancy of K^+ binding sites on the external surface in E_2 state. In deducing the mechanism of the active ion transport it is important to determine what effect the E_1 - E_2 state transition has on the structure of the pump molecule. Two-dimensional membrane-bound E_2 crystals can be induced by PO_4, CrO_4 or VO_3 ions. Here we report the crystallization of pure Na,K-ATPase from pig kidney outer medulla exposed to 5×10^{-6} to 10^{-5} M $PrCl_3$ in the presence of 0.1 M NaCl, 10 mM $MgCl_2$ and 10 mM Tris-Cl at pH 8.0. 2-D crystals are formed within 14 to 18 days. No crystallization is observed when K^+ is present. Therefore the lanthanide induced crystals presumably represent the conformation of the Na,K-ATPase in the E_1 state. Computerized image analysis, using the SPIDER program, shows that the symmetry of the lanthanide induced crystals is of P1 space group and the dimensions of the unit cell are: a = 60 Å, b = 58 Å and γ = 70 degrees, similar to the E_2 type crystals induced by $NaVO_3$. Three-dimensional reconstruction of the structure of Na,K-ATPase in the two crystal forms will provide information about the shape and density distribution of the hydrophilic portions of the molecule in the E_1 and E_2 states. (Supported by NIH grants GM 27804 and AM 26545.)

M-AM-I4 THE COUPLING OF NA-K ATPASE AND GLYCOLYSIS IN THE RENAL CELL LINE MDCK. R.M. Lynch and R.S. Balaban LKEM, NHLBI, NIH. Bethesda MD 20205. Spons. J.A. Ferretti

Previously we found that glycolysis was more sensitive than oxidative phosphorylation to alterations in Na-K transport in MDCK cells. We further investigated this interaction by measuring K^+ uptake via Na-K ATPase as a function of glycolytic activity. The number of pump sites also was determined using ^{3}H-ouabain. Medium K^+ concentration ($[K^+]o$) was monitored using a K^+ sensitive electrode. Unidirectional K^+ uptake was measured after the reintroduction of K^+ to K^+ depleted cells, incubated with or without glucose. All experiments were conducted in the presence of 2 mM glutamine. In glucose free media 11.7 ±0.5(SEM) moles of K^+ were transported per mole O_2 consumed, during the first 15-45 seconds after the readdition of K^+, corresponding to a K^+/ATP of ≈2.0. The initial rate of K^+ uptake was measured over a range of ($[K^+]o$), and Eadie-Hofstee analysis indicated a Km for K^+ of 3.0 mM with a Vmax of 69.0 nmol K^+/min mg protein. In the presence of glucose, the K^+/ATP was unaltered, whereas, the initial rate of K^+ uptake was increased at all $[K^+]o$. This increase was associated with a 52% increase in Vmax without a significant change in the Km for K^+. Steady state K^+ uptake was also increased in the presence of glucose based on steady state $[K^+]o$ determinations. In addition, no change in the number of ouabain binding sites was detected in the presence of glucose. These results demonstrate that the Vmax of each pump site has increased in the presence of glycolysis. The mechanism of this interaction is unknown. However, these results are consistent with a functional compartmentation of Na-K ATPase with glycolysis in the MDCK cell line.

M-AM-I5 VOLTAGE DEPENDENCE OF NA/K PUMP RATE IN SQUID GIANT AXON. David C. Gadsby, R.F. Rakowski and Paul De Weer. Marine Biological Laboratory, Woods Hole, MA 02543.

The Na/K pump is electrogenic, normally extruding more Na than the K taken up, so that the pump rate should be voltage-sensitive and decline with membrane hyperpolarization. Pump rate was estimated by measuring simultaneously the changes in membrane current and in ^{22}Na efflux caused by application of the cardiotonic steroid dihydrodigitoxigenin (H_2DTG, 10 μM) to voltage-clamped, internally-dialyzed giant axons of the squid, at the normal resting potential, -60 mV, and also at 0 mV. To fully activate the Na/K pump while minimizing K^+ currents, and so keeping holding currents small (+2 μA.cm^{-2}>I_m>-8 μA.cm^{-2}), seawaters were Na-free, containing 415 mM N-methyl-D-glucamine (NMG), 1 mM 3,4-diaminopyridine, and 10 mM K, and internal dialysis fluids were K-free, containing 190 mM NMG, 50 mM Na, 5 mM ATP, 250 μM veratridine to keep Na channels open, and were strongly buffered with 250 mM HEPES. Two additional voltage-clamp circuits kept the potentials of the central pool and end pools equal and so eliminated longitudinal current flow via the grease seals. Each axon was tested for the absence of such longitudinal current, by comparing tetrodotoxin-induced changes in ^{22}Na efflux and in membrane current, which should be identical in Na-free seawater. Fully bracketed data were collected in 5 axons, and the sizes of the H_2DTG-sensitive current and ^{22}Na efflux, obtained at -60 mV, relative to the corresponding values determined at 0 mV, averaged 0.55 ± 0.04 (S.E.M., n=10) for current, and 0.70 ± 0.04 for Na efflux, respectively, confirming that Na/K pump rate is voltage-dependent. USPHS grants: HL 14899, NS 22979, NS 11223.

M-AM-I6 Na/Na EXCHANGE ACTIVATED BY INTERNAL Ca IN SQUID AXONS. AN OPERATIONAL MODE OF THE Na/Ca EXCHANGE. R. DiPolo and L. Beaugé. IVIC, Venezuela. M.Y.M. Ferreira, Córdoba, Argentina.

In squid axons the Na/Ca exchange is highly asymmetric. Ca_i activates the reverse mode (Na_i:Ca_o exchange) of the exchange process. Ca_i not only promotes Ca_o-dependent Na efflux but also Na_o-dependent Na efflux (DiPolo and Beaugé. Biophys J. 1984). We have explored whether this ouabain insensitive Na/Na exchange is part of the operation of the Na/Ca exchange. Na_o and Ca_o-dependent Na efflux components were measured in internal dialyzed axons containing (mM): 310 K; 100 Na; 30 TRIS; 4 Mg; 1-3 EGTA; 310 Aspartate; 138 Cl; 100 glycine. The standard seawater (440 mM Na, 10 mM Ca) contained ouabain, cyanide and TTX. The results show: 1) Internal alkalinization (pH 8.5), known to activate the forward exchange (Na_o-dependent Ca efflux) (DiPolo and Beaugé. BBA 688, 237, 1982), also promotes Na_o-dependent Na_o efflux and to a lesser extent Ca_o-dependent Na efflux. This effect occurs in the presence of Ca_i. 2) Removal of Mg_i activates the Na_o-dependent Na efflux as well as the Na_o-dependent Ca efflux. 3) The activation of the Na/Na exchange by Ca_i ($K_{½}$=2-5 μM) as well as the activation of Na efflux by Na_o ($K_{½}$=110 mM) are low affinity processes. 4) Na_o-dependent Na efflux is inhibited by high Ca_o, suggesting competition between Na_o and Ca_o for external sites on the carrier. 5) Simultaneous measurements of Ca and Na effluxes (^{24}Na, ^{45}Ca) show that concurrent with the activation of the Ca efflux by Na_o, a sizable Na_o-dependent Na efflux also occurs. These results indicate the existence of a Na/Na exchange component dependent on Ca_i and present during the normal operation of the Na/Ca counter transport. This component should be taken into account in evaluating the stoichiometry of the Na/Ca exchange. (Supported by CONICIT. S1-1144, Venezuela and NSF BNS 8500595 USA).

M-AM-I7 CALCIUM-ACTIVATED Na EFFLUX IN SMOOTH MUSCLE. B.G. Kennedy, A.J. Wasserman, J.H. Kaplan, A.P. Somlyo, Dept. of Physiology, Univ. of Pennsylvania G4, Phila. PA 19104.

We have measured unidirectional-efflux of ^{22}Na in the presence and absence of Ca_o in smooth muscle strips of rabbit hepatic portal vein. The present results were obtained at 37°C in the presence of 10^{-4} M ouabain (to exclude any contribution from the sodium pump) and employed Na loaded muscle fibers ($Na_i \simeq 1200$ and $K_i \simeq 10$ mmole/kg dry weight). The composition of the modified Krebs solution was (in mM): 135 NaCl, 5 glucose, 1.2 $MgSO_4$, 10 HEPES, 1.2 Tris phosphate and 5 KCl, pH 7.4. Ca, when present was 1.2 mM; Ca-free solutions contained 2 mM EGTA. In the absence of Ca, the mean rate constant for ^{22}Na efflux was 0.08 (n=4, SEM=0.007) min^{-1}, and did not change significantly upon addition of Ca_o. When efflux was determined with isosmotic replacement of NaCl with LiCl the mean rate constant was 0.04 (n=9, SEM=0.002) min^{-1}. Addition of Ca to the extracellular LiCl medium caused an abrupt, large increase in Na efflux. The increase in rate constant was transient, peaking at about 4 X baseline level, with a half time to peak on the order of 1 min. This Ca-induced increase in unidirectional Na efflux was similarly observed with isosmotic substitution of K for Na, and was not inhibited by 0.1 mM amiloride. Na efflux into LiCl was accompanied by the cellular uptake of Li (700 mmol/ kg dry weight) and K (260 mmol/kg dry weight). The K uptake measured by electron probe X-ray microanalysis, was also activated by the addition of Ca_o. The Ca_o effect was absent in a K-free medium. Vascular smooth muscle cells contain a ouabain-resistant, K_o-dependent, Na_o-inhibitable Na efflux mechanism that is activated by Ca. Supported by NIH HL 15835 (to the Pennsylvania Muscle Institute), HL 30315, RCDA HL 01092.

M-AM-I8 RED CELL SODIUM PUMP MEDIATES ^{86}Rb UPTAKE IN THE ABSENCE OF PHOSPHORYLATION. L. J. Kenney and J. H. Kaplan. Department of Physiology G4, University of Pennsylvania Philadelphia, PA 19104

When human red cell ghosts are prepared in the absence of phosphate or nucleotides, a small uptake of ^{86}Rb is observed that occurs via the sodium pump. This ouabain-sensitive uptake of ^{86}Rb is stimulated by internal Rb and represents a Rb:Rb exchange that is ATP, ADP and P_i-independent. These fluxes represent a non-energized mode of the sodium pump acting as a simple facilitated diffusion system. The passive Rb:Rb exchange flux constitutes < 0.5% of the maximal Na:K exchange under saturating conditions. We have observed that in the absence of a phosphorylated intermediate (E_2P), high affinity sites for Rb exist on the external surface of the sodium pump (Km < 50 uM). At 50 uM Rb_o, the presence of 140 mM NaCl in the external medium inhibit ^{86}Rb uptake. Other monovalent cations, Cs, Li, K but not tris or choline will substitute for Rb at the cytoplasmic surface. The measurement of these fluxes enables the description of cation-cation interactions on sodium pump binding sites at the trans and cis faces of the pump in the absence of phosphorylation-dependent conformational transitions. Supported by NI HL 30315, RCDA K04 HL 01092 and CEll and Molecular Biology Training Grant 5T 32 GM 07229.

M-AM-I9 ERYTHROID CELL DIFFERENTIATION AND CHANGES IN AMINO ACID TRANSPORT. J.V. Vadgama, M. Castro, and H.N. Christensen, Dept. of Biol. Chem., Univ. of Michigan, Ann Arbor, MI 48109

We had recently postulated that the Na^+-independent transport System asc discovered in the nucleated pigeon red cell and specific for the transport of threonine, serine, alanine, and valine, may already be present as a biological entity in the nucleated mammalian erythroid cell stages (J.V. Vadgama and H.N. Christensen, J. Biol. Chem. 260, 2912, 1985). We are now examining the changes in amino acid transport in developing erythroid cells isolated from rat fetal liver at various stages of gestation. Our results show that at day 13 the fetal erythroid cells possess a significantly large saturable, Na^+-dependent uptake of 2-(methylamino)isobutyric acid (MeAIB). This activity declines as gestation proceeds and virtually disappears near term. In support of earlier reports, the mature red cell lacks Na^+-dependent transport of MeAIB attributable to System A. In comparison the saturable Na^+-dependent transport of threonine, presumably via System ASC, rises from day 14 to 16 and remains vigorous up to day 18. Soon after its activity declines, but remains conspicuously saturable. This component is, as usual for System ASC, MeAIB-insensitive. The expression of System ASC at such an early stage in fetal life and its small but sustained dominance at later stages of development suggests that perhaps the activity of this Na^+-dependent system plays an important role for the survival of erythroid cells. Saturable Na^+-independent transport of threonine, presumably by System asc, is slower but definitely present. This activity rises at day 18, but decreases after delivery. Inhibition results confirm its independence from System L, thus supporting our hypothesis for its presence as an independent biological activity. Interesting observations were made with other transport systems during different stages of erythroid cell differentiation. Support acknowledged from Grant HD01233, NIH, U.S.P.H.S.

M-AM-I10 ETHOXYFORMYLATION OF HISTIDINE ELIMINATES COOPERATIVITY OF CA^{2+} BINDING TO SR ATPase. Carol Coan, Dept. of Physiology, University of the Pacific, 2155 Webster St., San Francisco, CA 94115

Modification of a small population of histidyl residues (24nm/mg) by ethoxyformic anhydride (EFA) eliminates the cooperativity of Ca^{2+} binding to high affinity, activating sites on the Ca•Mg•ATPase of SR. Equilibrium binding studies using column chromatography yield non-cooperative binding curves with a total of 7-8nm Ca bound/mg protein. The best fit to Scatchard type plots is given by two independent sites with $K \approx .40 \times 10^{-6}$; $.55 \times 10^{-5}$, respectively. Loss of enzyme activity is concominant with histidine modification. EPR spectroscopy is used to monitor the conformation of the enzyme. An iodoacetamide spin label, covalently attached to the ATPase is specifically sensitive to a conformational change in the ATP hydrolysis site which accompanies Ca^{2+} activation. As with the non-modified enzyme, we find a one to one coupling between Ca^{2+} binding and the conformational change, titrations of EPR spectral parameters expressing the same degree of site independence. No evidence of denaturation is found in the EPR spectrum. Furthermore, the histidine modification is reversible with a large excess of imadazole at basic pH, and activity is recovered. In as far as the EPR spectra are indicitive, the "Ca activated conformation" can be achieved with EFA-ATPase when the Ca binding is finally complete. Thus, it does not appear that denaturation or alteration in the initial Ca•Enzyme•Substrate complex is responsible for loss of activity.

M-AM-I11 Na-DEPENDENT AMINO ACID TRANSPORT AS A MECHANISM FOR THE DECREASE IN INTRACELLULAR Na CONCENTRATION $(Na)_i$ DURING Me_2SO-INDUCED FRIEND MURINE ERYTHROLEUKEMIC (MEL) CELL DIFFERENTIATION. Deborah A. Lannigan and Philip A. Knauf, Dept. of Rad. Biol. and Biophys., Univ. of Rochester, Rochester, NY 14642

The earliest known ionic event during MEL cell differentiation along the erythroid pathway is a 40 percent drop in $(Na)_i$ due to a decrease in Na influx. This decreased Na influx was found to be: 1) insensitive to bumetanide or DIDS; 2) pH independent (using the weak acid DMO the pH in MEL cells was 7.23 ± 0.02 which did not change up to 15 h after Me_2SO induction by which time Na influx has decreased by ~ 40 percent); 3) not due to a change in membrane potential (the membrane potential as measured by TPP^+ influx did not change between uninduced and 15 h Me_2SO-induced MEL cells). The major source of the decreased Na influx was a drop in Na-dependent amino acid transport. Removal of amino acids from uninduced cells caused the Na^+ influx to drop from 9.33 ± 0.37 nmoles $Na^+/10^6$ cells-min to 5.30 ± 0.41 ($p < 0.01$, $N = 32$), a rate similar to that seen in cells induced for 15 h with Me_2SO (5.45 ± 0.34). In contrast, removal of amino acids from induced cells caused a much smaller decrease in Na^+ influx to 3.80 ± 0.61, which was not statistically significant ($p > 0.1$, $N = 22$), suggesting that a large fraction of the Na-dependent amino acid transport is lost during induction. Removing the amino acids from uninduced cells decreased $(Na)_i$ by approximately 34 percent, thus indicating that this mechanism could account for the majority of the change in intracellular Na^+ during induction. Supported by NIH grants HL 18208 and AM 27495.

M-AM-I12 INTERACTION OF TNP-ATP WITH THE GASTRIC H,K-ATPASE. Larry D. Faller (Intr. by David Eisenberg) CURE/UCLA, Wadsworth Veterans Administration Hospital Center, Los Angeles, CA 90073.

The fluorescent substrate analogue 2',3'-O-(2,4,6-trinitrocyclohexadienylidine) adenosine 5'-triphosphate (TNP-ATP) has been used to investigate the number of nucleotide binding sites and cofactor-induced changes in the structure of the potassium-stimulated, proton-translocating adenosine triphosphatase (H,K-ATPase) found in microsomal vesicles isolated from gastric mucosae. The fluorescence of TNP-ATP in aqueous solution is enhanced 6-fold by binding to the H,K-ATPase. The principal observations made in the study are as follows: First, TNP-ATP binds to a single class of sites on the apoenzyme with a stoichiometry of 3.4 ± 0.5 nmol mg^{-1} ($n = 11$). Second, the fluorophore can exist in at least three different protein-lipid environments. K^+ causes a rapid fluorescence quench by binding to a single class of sites with $K_d = 3$ mM. Rapid and complete reversal of the K^+-quench by Mg^{2+} is followed by a slow quench to a lower fluorescence level with $\tau_{\frac{1}{2}} \simeq 5$ min. TNP-ATP dissociation cannot account for the observed changes. Third, ATP displaces TNP-ATP from apoenzyme completely and monophasically. However, displacement of TNP-ATP from the Mg^{2+}-quenched state by ATP is biphasic. $K_{S1}(app) = 5.8 \pm 3.3$ μM and $K_{S2}(app) = 1.3 \pm 0.4$ mM ($n = 5$), giving estimates of $K_{S1} = 0.6$ μM and $K_{S2} = 130$ μM that are in reasonable agreement with published values of the Michaelis constants $K_{M1} = 0.4$ μM and $K_{M2} = 50$ μM under comparable conditions (Wallmark et al., J. Biol. Chem. 255, 5313, 1980). Fourth, TNP-ATP competitively inhibits K^+-activated hydrolysis of ATP at both high and low substrate concentrations. (Supported by NSF PCM83-09756 and NIH AM 17328-C2).